ADDIS ABABA UNIVERSITY

ADDIS ABABA INSTITUTE OF TECHNOLOGY

SCHOOL OF CIVIL AND ENVIRONMENTAL ENGINEERING

ASSESSMENT OF LOAD CARRYING CAPACITY OF ARCH BRIDGE-Case Study on Odie Bridge

A Thesis Submitted to School of Graduate Studies in Partial Fulfillment of the Requirement for Degree of Master of Science in Civil Engineering (Structures)

By Abiyu Awoke

June, 2020

Addis Ababa, Ethiopia

The undersigned have examined the thesis entitled **Assessment of Load Carrying Capacity of Arch Bridge: Case study on Odie Bridge**; presented by Abiyu Awoke Adgeh, a candidate for the degree of *Master of Science in Civil Engineering (Structures)* and hereby certify that it is worthy of acceptance.

Dr. Abrham Gebre		
Advisor	Signature	Date
Internal Examiner	Signature	Date
External Examiner	Signature	Date
Chair person	Signature	Date

UNDERTAKING

I certify that my research work entitled Assessment of Load Carrying Capacity of Arch Bridge Case study on Odie Bridge is my original work done under the supervision of my research advisor Dr. Abrham Gebre. The work has not been presented elsewhere for assessment. The material used from other sources has been properly acknowledged/referred.

Signature _____

Abiyu Awoke

ABSTRACT

Arch bridges possess an enormous capacity that can carry larger load than assessed through the application of limit state analysis and experimental methods. In the case of arch bridges, accessing detailed information of the structure is a bit difficult.

In this study, load carrying capacity of Odie bridge, which is non-reinforced concrete arch bridge found in Ethiopia Federal Road Network, is carried out. Nonlinear finite element analysis was adopted using the total strain crack model in Midas FEA. Arch Bridge can manage load even with the formation of hinges. The study is focused on identification of the formation of cracks in arch barrel due to its own weight and vehicular loads applied at the quarter and crown point of the arch. Moreover, an influence surface along the top surface of the bridge was generated. Using the influence surface, the vehicular axle load positions were identified. Crack formation and stress in the arch due to a moving load is captured.

To validate the numerical model, verification on Prestwood Bridge was used. The study revealed that the comparison between the numerical model and the full-scale test of Prestwood Bridge is applicable to estimate load carrying capacity of non-reinforced concrete arch bridges.

ACKNOWLEDGMENTS

First of all, I would like to thank the Almighty God, who I am highly indebted to, for giving me everything I need to finish this thesis on time. Next, I also would like to thank my thesis advisor, **Dr. Abrham Gebre,** for his continuous support**.** My gratitude goes to Midas IT Department for their continuous support.

Furthermore, I would like to thank everyone who had contributed to the successful completion of this thesis and a special thank to my wife, who helped and encouraged me during challenging times that I have faced.

TABLE OF CONTENTS

ABSTRACT ..... **III**

ACKNOWLEDGMENTS ..... **IV**

TABLE OF CONTENTS ..... **V**

LIST OF TABLES ..... **VII**

LIST OF FIGURES ..... **VIII**

CHAPTER 1 ..... **1**

1.1 Background 1

1.2 Statement of the Problem 1

1.3 Objective 1

1.3.1 General Objective 1

1.3.2 Specific Objective 2

1.4 Limitation of the Thesis 2

1.5 Organization of the Thesis 2

CHAPTER 2 ..... **4**

2.1 History of Arch Bridges 4

2.2 Arch Bridges in Ethiopia 5

2.3 Analysis Methods 6

2.3.1 Analytical Methods 6

2.3.2 Semi-Empirical Methods 13

2.4 Numerical Analysis (Software Programs) 15

2.4.1 3D Non-Linear Finite Element Model Systems 15

CHAPTER 3 ..... **17**

3.1 Construction of the bridge 17

3.2 Maintenance history of the bridge 19

3.3 Inspection of the bridge 20

3.4 Dimensions of the Odie Bridge 20

3.5 Compressive strength of Concrete 21

CHAPTER 4 ..... **22**

CHAPTER 5 ..... **25**

5.1 Finite Element Model Using Midas FEA 25
5.2 Validation 25
5.3 Odie Bridge 29
5.4 Modeling of the Bridge of Odie Bridge 32
5.5 Loading 33
5.6 Analysis 34
CHAPTER 6 37
CHAPTER 7 42
7.1 Conclusion 42
7.2 Recommendation 42
REFERENCES 43
APPENDIX A 45
APPENDIX B 47
APPENDIX C 50
APPENDIX D 51

LIST OF TABLES

Table 3-1: Characteristic Compressive Strength of the Concrete Sets.....21
Table 5-1 Material Properties of arch Concrete 32
Table 5-2 Material Properties of Backfill.....33

LIST OF FIGURES

Figure 2-1 Pont du Gard Aqueduct, France (Chen and Duan) 4
Figure 2-2 Zhao Zhou Bridge, China (Qian,1987) 5
Figure 2-3 Geometry models in maximum stress analyses: 3-pin (a, b), 2-pin (c) and fixed-end arch rib (d) (Sustainable Bridges SB4.7.3) 8
Figure 2-4 Location and variation of thrust line and Zone of Thrust in segments. (Sustainable Bridges SB4.7.3) 9
Figure 2-5 Stress Block in the Zone of Thrust (Sustainable Bridges SB4.7.3) 11
Figure 2-6 Collapse Mechanism of an Arch (Heyman J.) 13
Figure 2-7 Arch Dimension and Description (ERA Bridge Design Manual 2013) 14
Figure 2-8 Nomogram for Determining the Provisional Axle Loading of Masonry arch bridge before factoring 15
Figure 3-1 Bridge Profile of Odie Bridge (ERA BMS, 2010) 18
Figure 3-2 The Odie Bridge 19
Figure 3-3 Reconstruction of the part of the parapet wall 19
Figure 3-4 Damage by vehicle Collison on Parapet walls 20
Figure 3-5 Odie Bridge Geometry 20
Figure 4-1 Hordijk Tension Softening Curve (Midas FEA, 2016) 23
Figure 4-2 Thorenfeldt Compression mode for Concrete (Midas FEA, 2016) 23
Figure 5-1 Prestwood Bridge before Collapse (Sustainable Bridges SB4.7.3) 26
Figure 5-2 Geometry of Prestwood bridge (Page ,1987) 26
Figure 5-3 FE Model of Prestwood Bridge. 27
Figure 5-4 Prestwood Bridge: Mechanism (Page,1987) 28
Figure 5-5 Vertical displacements of Point Under loading for Prestwood Bridge 28
Figure 5-6 Boundary Condition of Odie Bridge 29
Figure 5-7 Influence surface for solid stress at the Springing point 30
Figure 5-8 Influence surface for solid stress at the Quarter point 30
Figure 5-9 Influence surface for solid stress at Crown 30
Figure 5-10 Final discretization using Auto-Mesh Finite Element Model of the Bridge. 31
Figure 5-11 Truck Type 3 Unit Weight = 227 kN 33
Figure 5-12 Truck Type 3-2 Unit Weight = 325 kN 33
Figure 5-13 Truck Type 3-3 Unit Weight = 364 kN 34
Figure 5-14 Loading at Quarter Point, Legal Truck Type-3 34

Figure 5-15 Loading at Crown, Legal Truck Type-3 35
Figure 5-16 Loading at Quarter Point, Legal Truck Type-3-2 35
Figure 5-17 Loading at Crown, Legal Truck Type-3-2 35
Figure 6-1 Hinge No.1 at Quarter Point, Legal Truck Type 3, Total Axle Load= 2824.87kN at 11^{th} Load step 37
Figure 6-2 Hinge No.2 at Right Springing Point, Legal truck Type 3, Total Axle Load=4622.52 kN at 18^{th} Load step 38
Figure 6-3 Hinge No.3 at Three Quarter Point, Legal truck Type 3, Total Axle Load=6163.36 kN at 24^{th} Load step 38
Figure 6-4 Hinge No.4 at Left Springing Point, Legal truck Type 3, Total Axle Load=6933.78kN at 27^{th} Load step 38
Figure 6-5 Vertical Displacement of quarter-point on arch under the Load for Legal Truck Load type 3 39
Figure 6-6 Hinge No.1 at Load at Crown, Legal Truck Type 3, Total Axle Load=6676.97kN at 13^{th} Load step 40
Figure 6-7 Hinge No.2 at Springing, Legal Truck Type 3, Total Axle Load= 13353.97kN at 26^{th} Load step 41

CHAPTER 1

INTRODUCTION

1.1 Background

According to the 2010 ERA Bridge Management System (BMS) Database there are approximately 600 masonry and concrete arch highway bridges that are found in Ethiopia road network according to the 2010. Almost all of these bridges were constructed in the late 1930's and are found to be in poor condition (ERA BMS,2010).Therefore, estimating the load carrying capacity of arch bridges using the recommendations given in Ethiopian Roads Authority Bridge Design Manual (ERA BDM,2013) is necessary.

1.2 Statement of the Problem

In order for arch bridges to keep serving for their intended design life and beyond, its components should be assessed and well understood. In this regard, crack in arch barrel of an arch have a decisive role that compromise their serviceability and strength feature. Formation of cracks in the concrete undermine the engineering characteristic of load bearing component by deteriorating the stiffness. Due to the lack of proper understanding of the load carrying capacity of arch bridges, their assessment often is not carried out rather destined to be replaced or demolished. Therefore, a thorough assessment of crack formation should be conducted to estimate the safe load carrying capacity of arch bridges. The assessment of arch bridge will ultimately affect the decision making that will not compromise the safety of the users and saving increased cost incurred by their owners.

1.3 Objective

1.3.1 General Objective

The research described in this thesis aims to develop a numerical model for estimating the load carrying capacity of arch bridge using a finite element analysis and extend the procedure in determining the safe load carrying capacity of arch bridges found in the federal road network of Ethiopia.

1.3.2 Specific Objective

The specific objectives of this research study are outlined below:

1. To provide accurate load estimation method that represent the complex, nonlinear relationship between the constituent materials and compressive strength of concrete subject to an incremental stepped loading
2. To model the process using Midas FEA software and
3. To provide a comparison study to validate the assessment method.

1.4 Limitation of the Thesis

Due to the complexity and nature of the problem, the spandrel walls are not treated in this study. In addition, the analysis is done only for the own weight of the bridge and moving loads.

1.5 Organization of the Thesis

The thesis is organized in seven chapters.

Chapter 1 gives an introductory content that shows the aim of the thesis, limitation of the study as well as the structure of the thesis.

Chapter 2 focuses on a detailed literature review where it covers the history of the design and construction of arch bridges in Ethiopia and the world. In addition, this chapter covers the different methods of load carrying capacity assessment methods by different researchers, designers, and engineers.

Chapter 3 describes the studied bridge in relation to geometry and material properties. Some findings on the bridge regarding maintenance or rehabilitation history, adaptations made to the bridge is discussed.

Chapter 4 tries to present the failure criteria set to evaluate the response of the studied bridge that is to be used in the analysis and result extraction.

In Chapter 5, the method and approach used in the modeling and analysis of the three-dimensional model by using Midas FEA general-purpose software is discussed. A

validation of the method analysis used in this study is explained and illustrated in this chapter.

Chapter 6 deals with the result and discussion. Here the results from the Midas FEA software are analyzed and interpreted.

The last chapter gives conclusions and recommendations drawn from the study.

CHAPTER 2

LITERATURE REVIEW

2.1 History of Arch Bridges

The application of arches to bridge structures came much later than girder and suspension types, but an arch is the first and greatest of Man's inventions in the field of structures because arch transfers loads relating distinctively to its shape. The Sumerians, a society that lived in the Tigris-Euphrates Valley, used sunbaked bricks for their main building material. To span an opening, they relied on corbel construction techniques. Around 4000 BC, they discovered the advantages of arch shape in construction and began to build arch entranceways and small arch bridges with their sunbaked bricks (Steinman and Watson, 1941).

Other communities with access to stone soon began to build arches with stone elements. By the time of the Romans most bridges were constructed as stone arches, also known as masonry or voussoir arches.

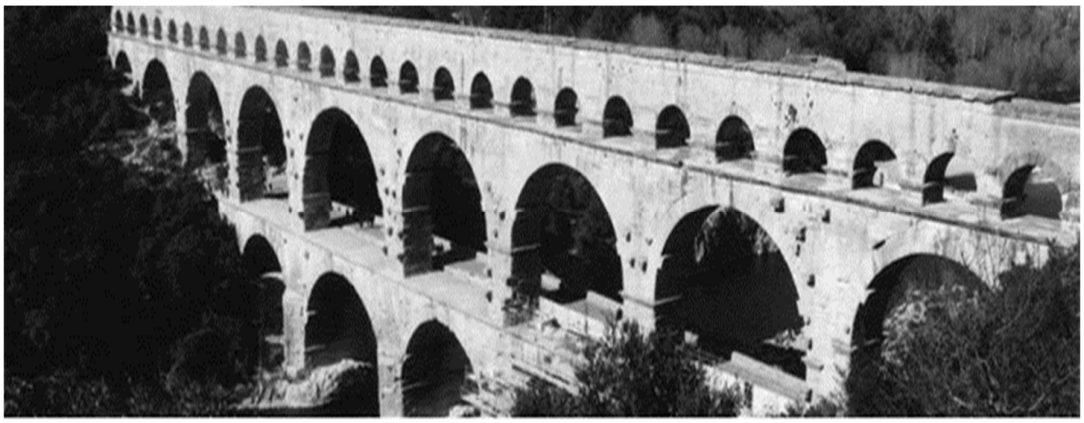

Figure 2-1 Pont du Gard Aqueduct, France (Chen and Duan)

Empirical rules were developed for dimensioning the shape of the arch and the wedge-shaped stones. The Romans were magnificent builders and many of their masonry bridges are still standing. Probably the most famous is the Pont du Gard at Nîmes in France (Figure 2-1), which was built shortly before the Christian era to allow the aqueduct of Nîmes (which is almost 50 km long) to cross the Gard River. The Roman architects and hydraulic engineers, who designed this bridge almost 50 m high with three levels, created a technical

as well as an artistic masterpiece. Excellent descriptions of other great Roman bridges can be found in Steinman and Watson. (Steinman and Watson,1941).

In China, ancient stone arch bridges with many shapes and configurations are ubiquitous. The Zhaozhou Bridge (Anji Bridge) shown in Figure 2-2 completed in 605 AD is the first shallow segmental stone arch bridge and the first open-spandrel arch bridge in the world(Qian ,1987).

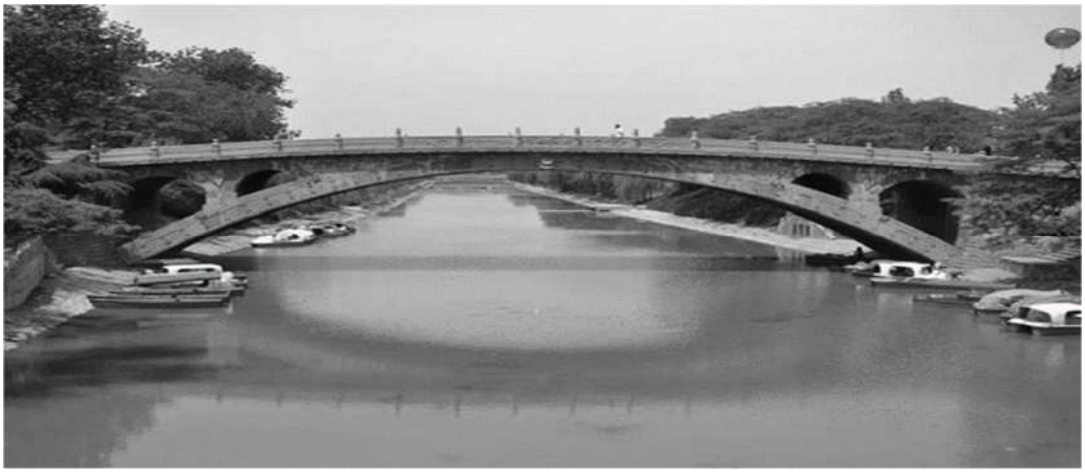

Figure 2-2 Zhao Zhou Bridge, China (Qian,1987)

2.2 Arch Bridges in Ethiopia

A safe and efficient transport system is fundamental to the freedom, wellbeing, and prosperity of a society. By their nature, bridges are essential elements in the road transport networks of Ethiopia and are vital to their operation. Restrictions to the operation of bridges or their closure can have effects beyond the immediate local disruption, including undesirable health and safety, economic, environmental, and political consequences.

Until the launch of the Road Sector Development Program by Ethiopian Roads Authority, many of the roads were constructed in the time of the Italian invasion where the dominant proportion of bridges used for the crossing of obstruction, valleys, waterways, or stream were of stone masonry and unreinforced concrete Arch bridges(http://www.era.gov.et).

Today the transport network in Ethiopia, as in many other countries, is under constant pressure to expand and increase capacity, with related economic and environmental costs. In this situation, the existing infrastructure must be used efficiently and to its full capacity.

Careful management of existing bridge assets can only achieve this. Changes in the requirements of the transport system and the gradual deterioration of existing structures in service mean that there is a growing need to maintain, repair, widen, and strengthen bridges over the coming decades. The success of this will be dependent on accurately determining the needs of bridges, understanding how best to undertake and allocate resources for their maintenance, repair, and renewal (ERA BMS,2010).

Masonry arch bridges can be viewed as among the most sustainable structures ever to have been built. Many have already been in service for more than 70 years without significant or no repair or strengthening works exceeding the design life requirements of modern structures (ERA BMS,2010).

2.3 Analysis Methods

The study of masonry arch has been performed for hundreds of years. The design of arches was based on the collapse mechanism and the thrust line following the shape of the arch so that there is either no bending moment or a reduced bending moment in the arch member. The shape of an arch can only satisfy one condition of loading without bending moments being developed. Temperature changes creep, foundation movements and imperfections must, however, introduce some bending in all but the three-hinged arch. In a bridge structure, live loading will produce a varying distribution of loading which will introduce bending. Clearly, the higher the proportion of dead loads the more nearly can the arch be designed to be in pure compression.

To determine the load carrying capacity of masonry arch bridges, different analytical and empirical methods give different results as well. Some empirical methods give approximate values of the load carrying capacity. However, these methods are also based on experimental techniques like laboratory tests or field tests. They usually have a form of simple formulae. Example Military Engineering Experimental Establishment (MEXE) method (ERA Bridge Design Manual, 2013).

2.3.1 Analytical Methods

As arches were the oldest structural systems used in buildings and bridges, understanding their complex structural behavior was a great task. Afterward, the 17th-century arches subjected to concentrated load were studied continuously rather than following the trial

and error approach. Failure of masonry arch can take various ways; it might result from material failure (Compressive or crushing), bond failure (Joint Opening), or formation of plastic hinge that will lead to the mechanism failure. Movement at the springing abutment can sometimes lead to failure in the above forms.

In order to analyze, any structural system developing a suitable analytical model producing the behavior of the subject form and loading is required. In the case of an arch, numerous models have been developed for centuries ranging from the classical elastic methods to the recent finite element methods.

Even though there are modern methods like finite element, engineers or designers still tend to use simple methods to evaluate or assess the loading carrying capacities of the arch under current traffic loading.

2.3.1.1 The Maximum Stress Analyses

The basic principle behind the use of stress analysis is to compare the results to the material properties that could serve the purpose without exceeding the limiting values. Several numerical models can be developed depending on the nature of the geometry, the effort needed for computation, and the required level of accuracy. Here the maximum stress values are sought that are of main concern, as there are limit states. These methods relate mainly to single-span bridge structures or to multi-span structures treating each span individually. Besides in its basic form, it is only analyzing a bare arch neglecting the influence of the backfill. A possible way of considering soil influence is introducing additional springs modeling lateral earth pressure proposed. (Martín-Caro et al, 2004)

This is a simple approach to analyze masonry arch spans by treating them as an arch rib made of an elastic material. These assumptions make the solution procedure a typical problem of a static calculation. Such a method gives reasonable results in cases when the stresses resulting from the loads are relatively lower than the material strength.

The selection of a method for solving a given problem depends on statically determinacy of the considered model. If it is statically determinate, (Figure 2-3(a)) it can be solved formulating equilibrium equations for horizontal and vertical forces and bending moments. However, in the case of a structure model that is statically indeterminate (Figure 2.3(c), (d)) it is solved generally employing integration of equilibrium equations, force method, or displacement method.

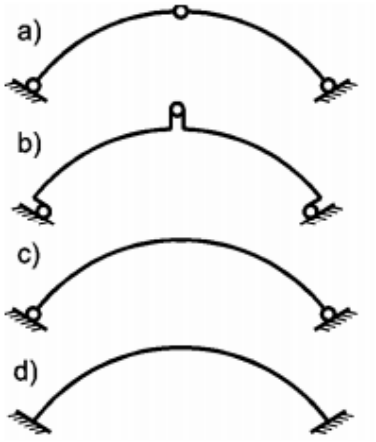

Figure 2-3 Geometry models in maximum stress analyses: 3-pin (a, b), 2-pin (c) and fixed-end arch rib (d) (Sustainable Bridges SB4.7.3)

In case of 2-pin arch scheme (Figure 2.3(b)), the problem can be reduced to the determination of the horizontal force, H from (the bending moment in the cross-section of the arch barrel, M , modulus of elasticity of the material, E, a moment of inertia of the arch barrel cross-section, I and the displacement y as a function of distance, s) component at springing from Eq 2-1:

$$H = \frac{\int \frac{M^P(s)y(s)}{EI(s)} ds}{\int \frac{y(s)^2}{EI(s)} ds} \qquad \textbf{Eq 2-1}$$

Where,

H is the horizontal force

Mp is the bending moment

I is the moment of inertia of the section

E is the modulus of elasticity and

Y is the vertical displacement

The inelastic arch rib methods accommodate the possibility for taking into account non-linear behavior of the arch material i.e. no resistance in tension and elastic-perfectly brittle or elastic-perfectly plastic behavior in compression. The concept proposed (Brencich et al, 2004) is based on static calculation as the above method however it involves the incremental procedure for loading and responding modification of the static scheme of the model during the analysis.

The whole structure is divided into segments and calculations are carried out in the nodes arising from the division. At every step of the solution procedure, an increment of the load is applied and elastic analysis is performed giving as a result of internal forces in the nodes. Then the height of the effective thickness x_i of a section is calculated from the average values of internal forces for both the section nodes. The effective thickness is established according to the assumed approach i.e. neglecting the tensile zone and/or the crushed area. In the next step, the geometry of the arch is updated: the section heights are equal to values of x_i and their axes are offset suitably (Figure 2-4). The entire length of the arch rib will be analyzed in this procedure. The connections between the ends of adjacent segments are infinitely rigid (Selby and Vecchio, 1993).

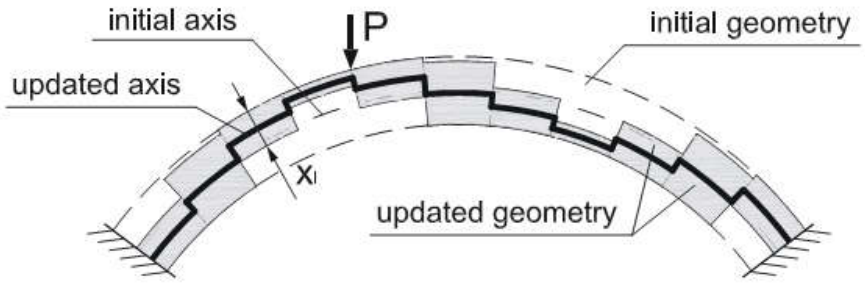

Figure 2-4 Location and variation of thrust line and Zone of Thrust in segments. (Sustainable Bridges SB4.7.3)

2.3.1.2 The thrust line analyses

The thrust line analysis controls the location and slope of the thrust line within the arch barrel. The analyzed parameter describing the location of the line of thrust can be an eccentricity of the force resultant e, being a function of normal force N and bending moment M acting in a considered cross-section. The slope of the thrust line is controlled by means of a relationship between normal force N and shear force T. Depending on the assumed theory and material model there are various limits for the line of thrust position. Structure meeting these conditions for given loads is assumed to be safe

"The middle third rule" the earliest version of the line of thrust impose or restricts the location of the resultant within the middle third of the section preventing tension to develop. This criterion has been arrived from elastic theory. Such a strict limit makes the method extremely conservative and at the same time is very difficult to achieve. It can be

satisfied only in cases when the structure has been properly designed and the dead loads considerably dominate live loads.

Relaxing the above limit the “middle half rule” was in place increasing the section allowed for compression reaching to reach half of the core.

The later limit of the method was proposed by Heyman 1966. He concluded that even if the line of thrust runs outside the allowed core in one section it does not threaten the safety of the whole structure. A structure will collapse only if the line of thrust reaches the edges of the arch barrel at least in four sections that would convert it into mechanism. According to this idea, the allowed space for the thrust line is the whole section of the arch barrel what can be written as:

$$e = \left|\frac{M}{N}\right| \leq \frac{d}{2} \qquad \textbf{Eq 2-2}$$

Where,

M is the bending moment
N is the thrust
d is the cross-section thickness

In the last approach, an important assumption is an infinite material compression strength, which enables the line of thrust to lie just at the edge of a cross-section. This presumption is rather not realistic but in most masonry bridge structures mean stresses are relatively low and the real solution is very near to the one obtained in this way (Sustainable Bridge SB7.4.3).

All the variants for the thrust line location can be summarized by employing the so-called ‘geometric factor of safety’ (Heyman, 1966). This factor is defined as the ratio between the actual arch barrel thickness and the minimum thickness of a similar arch accommodating the line of thrust from a given set of loads. According to this definition, a structure with a load giving the thrust line satisfying the limit of “middle third rule” has a geometric factor of safety equal to 3(Sustainable Bridge SB7.4.3).

2.3.1.3 Zone of thrust

This method is similar to the line of thrust analysis with the only difference where limit over the indefinite strength of the material is imposed. Here the material compressive strength is definite and limited. The position of the resultant cannot be at the edge of the arch rib rather a rectangular area with the arch section.

It is based on the elastic-plastic material model. The method permits the creation of a rectangular 'yield block' around the point of the force resultant position (Figure 2-5). According to the method assumptions, the force resultant lies in the middle of that yield area. The height of the yield block **t** is equal to the minimal one providing transmitting the normal force **N** at the given material strength f_c and an arch barrel width **B** what can be written as:

$$t = \frac{N}{f_c . B} \qquad \text{Eq 2-3}$$

Where,

N is normal force

fc is material compressive strength

B is barrel width

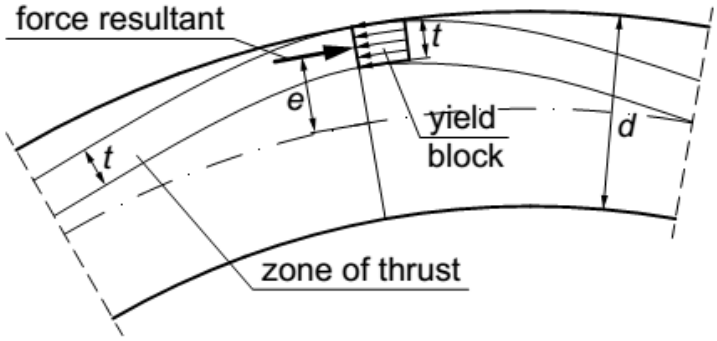

Figure 2-5 Stress Block in the Zone of Thrust (Sustainable Bridges SB4.7.3)

The resultant force at every section of the arch shall not be close to the edge less than half of the yield block, **t**/2. This controlled the failure of the arch from going into mechanism. (Sustainable Bridges SB4.7.3)

$$e = \left|\frac{M}{N}\right| \leq \frac{d - t}{2} \qquad \text{Eq 2-4}$$

Where,

M is the bending moment

N is the normal force

d is thickness of cross section

t is the yield (compression) block depth

2.3.1.4 The Mechanism method

The mechanism method is a kinematic approach where it assumes the formation of enough hinges for collapse. A specific approach to the analysis of masonry arches presents a group of the mechanism methods. On the contrary, to the previously mentioned lower bound analyses, these methods are based on the upper bound approach and hence are used only in a limit analysis giving a load carrying capacity and a failure mode of a structure. The algorithm of the methods applies to the kinematic approach. It uses an assumption, which has been confirmed in numerous experimental tests, that a masonry arch becomes a mechanism when at least four plastic hinges appear it the arch barrel (Heyman, 1966). However, the position of the hinges is unknown and hence it has to be assumed or calculated.

One of the most representative methods developed during the eighteenth century was couplet's Mechanism Method (Heyman, 1966). His contribution was outstanding with clear ideas about the line of thrust and mechanisms of collapse caused by the formation of hinges. Later in the last quarter of the eighteenth century, a young man called Coulomb concluded that if friction is high preventing sliding between blocks the only possible mode of failure is the formation of hinges in the arch rib (Heyman, 1966). In his conclusion, Coulomb stated for equilibrium to be satisfied one should keep the line of thrust within the arch rib that will ensure stability for a given loading situation.

In a simplified approach, the positions of the first three hinges under a single concentrated load can be assumed to be one right under the load and the other two at springing (Abutments). Looking for the best mechanism mode various hinge locations should be taken until the minimum load is found that would result in a mechanism. This could be achieved by equilibrium seeking moment at the hinges at an arbitrary location on the arch equating it to zero or with the equation of virtual work method (Sustainable Bridges SB4.7.3).

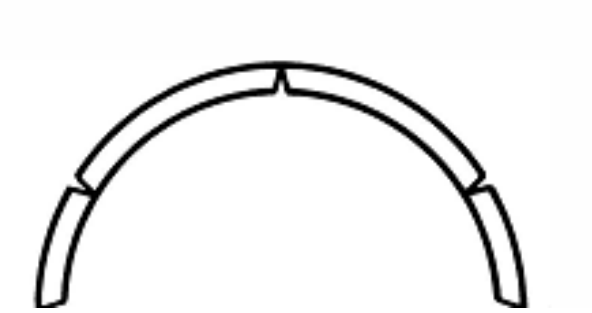

Figure 2-6 Collapse Mechanism of an Arch (Heyman J.)

2.3.2 Semi-Empirical Methods

2.3.2.1 MEXE method

The MEXE (Military Engineering Experimental Establishment) method is a semi-empirical method, which was developed during the Second World War. This method was traditionally used to determine the capacity appraisal of masonry arch bridges. The MEXE method comprises the calculation of a provisional axle load (PAL) that relates to the performance of a 'standard' arch barrel using either a nomogram given in Ethiopian Road Authority (ERA) Bridge Design Manual: for Determining the Provisional Axle Loading of Masonry Arch Bridges before Factoring or the equation:

$$\boldsymbol{PAL = \frac{740(d+h)^2}{L^{1.3}}(tonnes)} \qquad \textbf{Eq 2-5}$$

Where:

PAL is the provisional axle load

d is crown thickness

h is height of fill above crown

L is the arch span

This is an idealized load; it is valid for structures satisfying the assumption that the arch span has a parabolic shape and is in the ideal condition. However, the method provides also the load carrying capacity for differently shaped and deteriorated structures. The modified MEXE method is a comprehensive method for determining the carrying capacity of single-span stone and masonry arches in terms of allowable axle weights. The method as such is concerned solely with the strength of the arch barrel and takes account of the materials, various defects, and geometric proportions, which affect the strength of the arch.

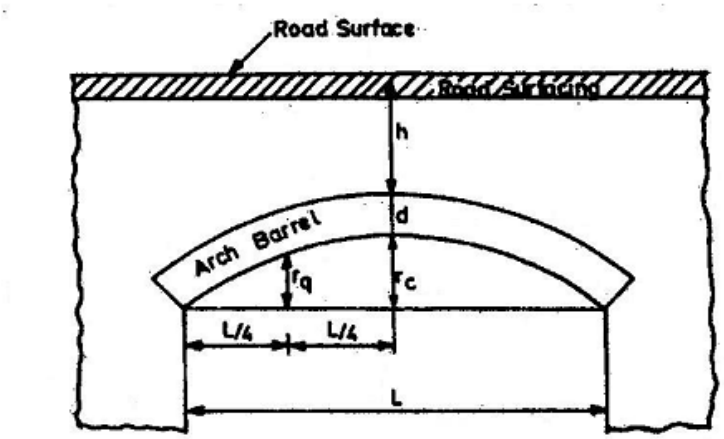

Figure 2-7 Arch Dimension and Description (ERA Bridge Design Manual 2013)

The provisional axle loading PAL is obtained by reference to the nomogram in Figure 2-8. Mark the arch span L on Column A and the total crown thickness (d + h) (where d is barrel and h is fill height) on Column B. Line through these points to Column C, and read off the provisional axle loading assessment in tones. Alternatively, the provisional axle loading shall be obtained by substituting the values of (d + h) and L in the above equation 2.5. The maximum value should not exceed 70 in the case of PAL determined from the equation Eq 2-5 (ERA Bridge Design manual, 2013).

After determining PAL (Provision axle load) factors accounting for the material properties, the condition of the bridge and geometric parameters like the ratio of the span to rise ration will be applied.

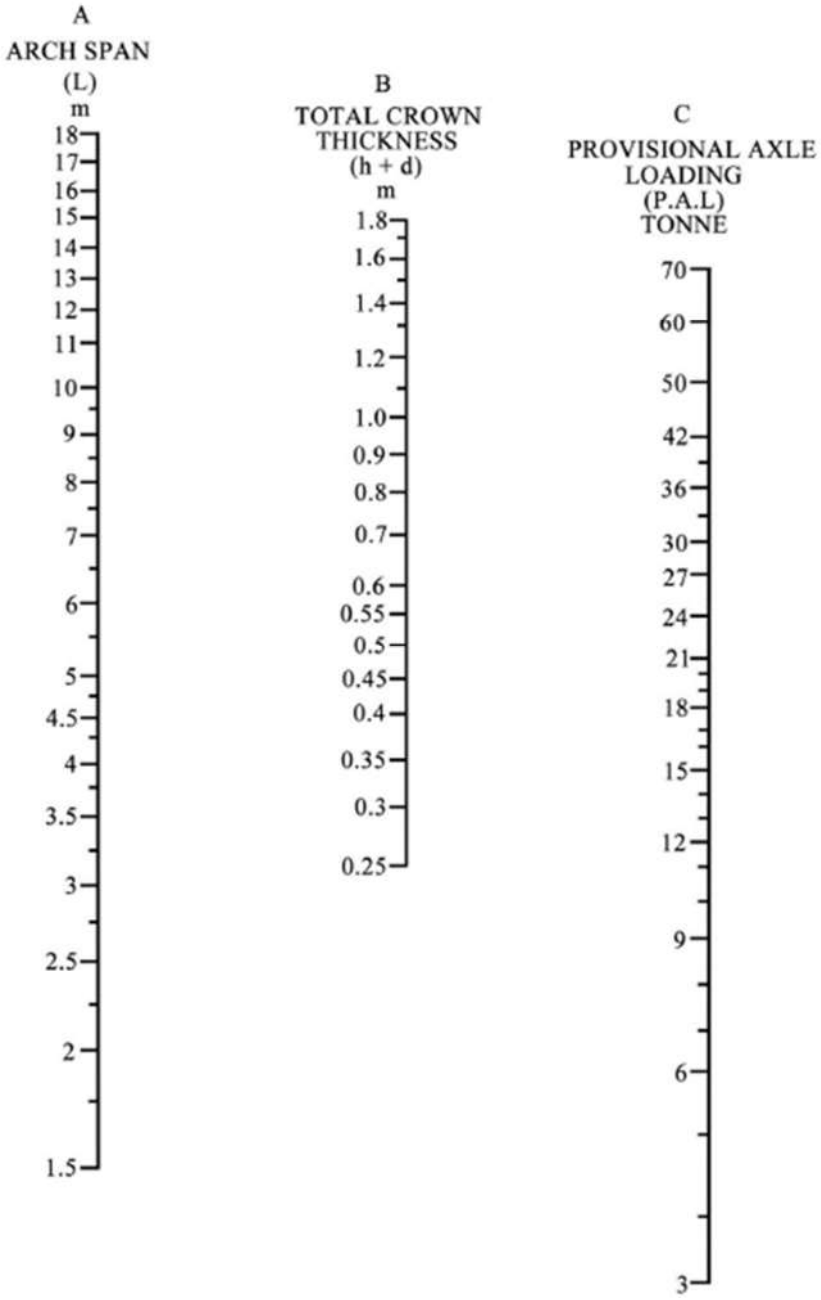

Figure 2-8 Nomogram for Determining the Provisional Axle Loading of Masonry arch bridge before factoring

2.4 Numerical Analysis (Software Programs)

2.4.1 3D Non-Linear Finite Element Model Systems

The finite element method (FEM) can be a program that is developed to handle the analysis of any type of structure. The use of FEM can be most appreciated when the modeling is

done in the utmost care and in a good way. Depending upon the type of the problem, one, two or three-dimensional elements can be used to model the given problem. As the model construction is the difficult and time-consuming routine activity in FEM, care must be exercised to achieve a more refined model with a shorter computational time that will create a balance in our model. The FEM makes use of different material properties modeled together that could help study the behaviors of each element in the model as needed. More complex modeling approaches are usually indispensable for considering some types of defects but on the other hand, sometimes increasing the dimension of elements does not give any additional information. That is why the right selection of the modeling technique is crucial (Sustainable Bridges SB4.7.3).

The methods mentioned earlier have been widely used for analyzing arch bridges because no complicated computations are required. However, those methods were based on many assumptions, which might affect the overall results of the ultimate load carrying capacity of the bridge.

The main advantage of the finite element analysis is the opportunity to model a whole structure including spandrel walls, wing walls, and abutments. To check the structural vulnerability only the behavior of the arch is considered but also the backfill and abutment are also analyzed. Additional modes of failure like longitudinal cracking of the arch barrel or spandrel walls separation cab be predicted. In terms of loads, further to static loads, dynamic and seismic loads can be implemented in the FEM. This also allows for differential settlement and soil-structure interaction (Sustainable Bridges SB4.7.3).

CHAPTER 3

DESCRIPTION OF STUDIED BRIDGE

The bridge under investigation is found on a road which is part of the Ethiopian Roads Authority federal road network, that connects the town of Komobolcha to Mille town. According to the Ethiopian Roads Authority Bridge management database (ERA BMS, 2010), the bridge is identified as Bridge No. B11-01-015. It was constructed during the Italian occupation 1939(ERA BMS ,2010). The bridge construction industry was a new introduction to the country as the main construction material was concrete which is not practiced mainly in Ethiopia prior to the Italian occupation. The bridge was constructed out of plain concrete without having reinforcements (ERA BMS,2010).

The bridge is a single-span arch with a stone masonry spandrel wall and backfill. The bridge has two-lanes with an out-to-out width of 9m, and a carriageway width of 7m, having a span of 22.50m. The thickness of the concrete arch rib/barrel is 1.40m and resting on stone masonry abutment which is founded on basaltic rock. There is no record of design nor working drawings for the bridge.

3.1 Construction of the bridge

Odie bridge was constructed out of plain concrete [evidence observed on demolished or collapsed arch bridges of similar nature and year of construction along the Kombolcha - Bati-Mile Road] dominantly with an aggregate of relatively larger size compared to the construction material choice practiced these days. At the time of the Italian annexation of Ethiopia, the road construction using locally available material was utilized.

Odie bridge abutments were constructed using poorly dressed stones with varying sizes. The spandrel walls were also poorly dressed stones cemented in mortar that rest on the extrados of the arch rib. The approach wing walls on both sides of the bridge are cemented stone masonry walls. The parapet walls on both sides of the bridge are extension of the spandrel wall made of a cemented stone masonry wall with a thin layer of mortar coping.

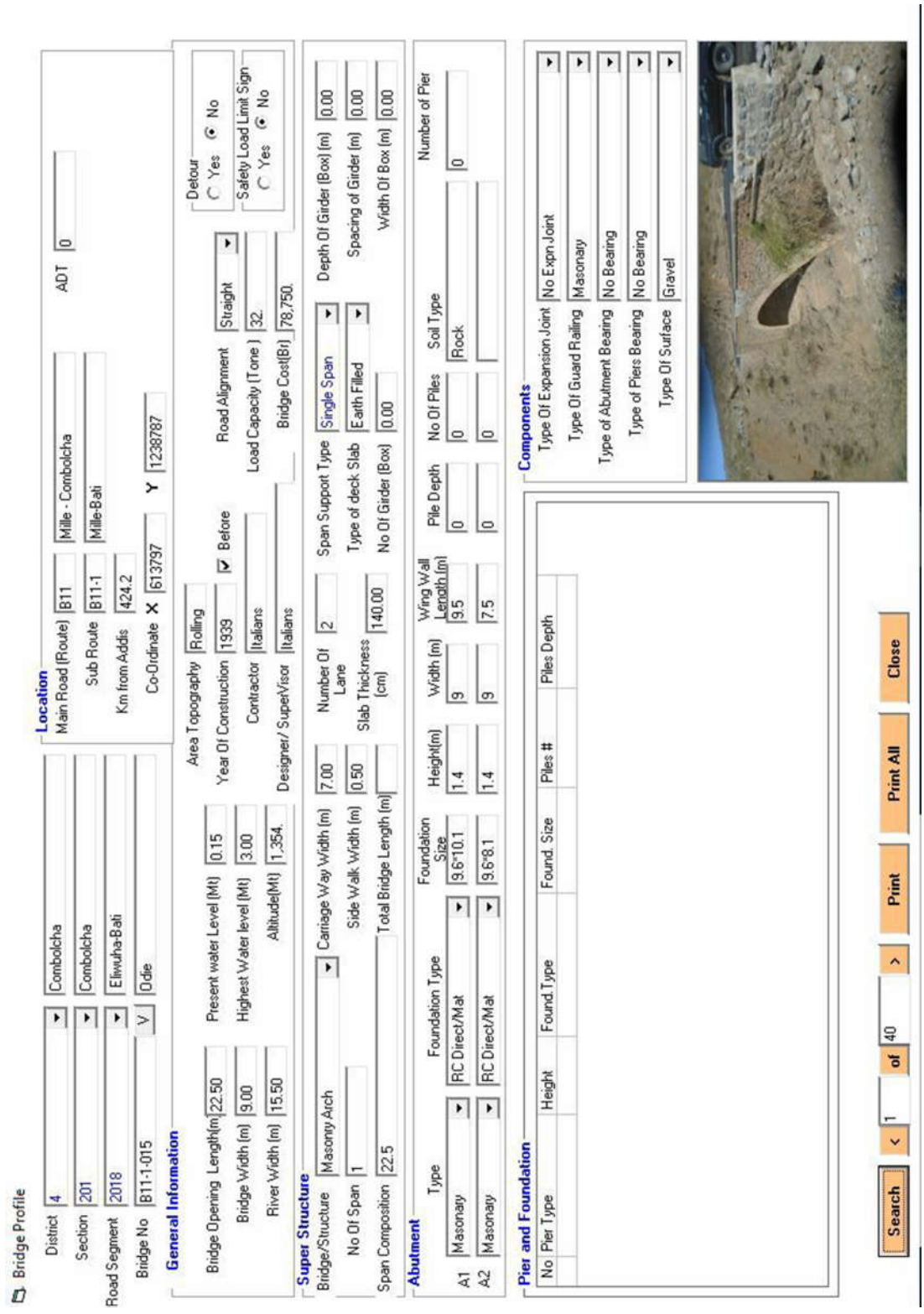

Figure 3-1 Bridge Profile of Odie Bridge (ERA BMS, 2010)

Figure 3-2 The Odie Bridge

3.2 Maintenance history of the bridge

As per Ethiopian Roads Authority Bridge Management System 2010 (ERA BMS,2010), no major maintenance or repair history is found expect for additional bituminous surfacing and reconstruction of part of the parapet wall (ERA BMS,2010).

Figure 3-3 Reconstruction of the part of the parapet wall

3.3 Inspection of the bridge

During inspection, it is observed that few areas of the intrados were deteriorated due to aging and effloresce effect. Moreover, damage to the parapet wall due to vehicles collision has been observed.

Figure 3-4 Damage by vehicle Collison on Parapet walls

3.4 Dimensions of the Odie Bridge

The detailed dimension of the bridge is shown in Figure 3-5.

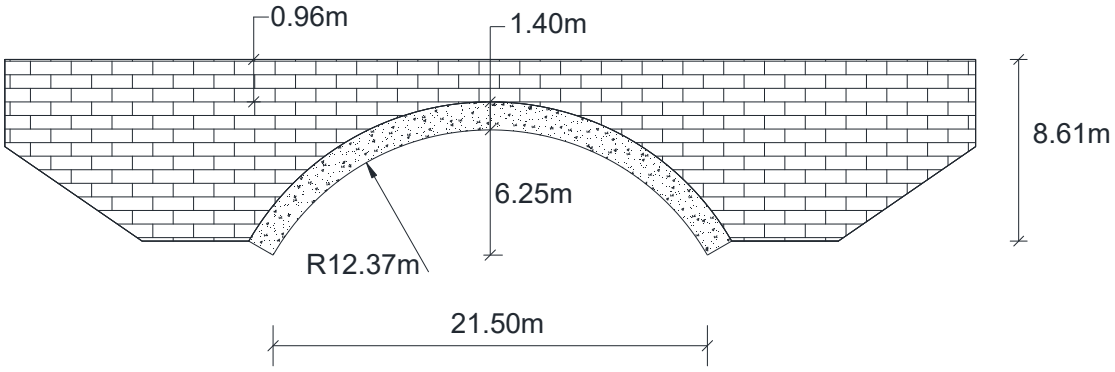

Figure 3-5 Odie Bridge Geometry

3.5 Compressive strength of Concrete

Due to a lack of design and related documents of the bridge, a survey to assess the residual strength of the bridge materials was done using a non-destructive test. For the capacity assessment of the bridge, the compressive strength was one of the center points of interest. The measured rebound strength test was tabulated under Appendix A. The characteristic compressive strength of the five sets of tests were calculated using probabilistic approach with 5 % of the population of all possible strength determinations of the volume of concrete under consideration, are expected to fall. (Eurocode EN1991-1, 2000, EN206-1, 2002)

Table 3-1: Characteristic Compressive Strength of the Concrete Sets

Set	Characteristic Strength, MPa
1	65.636
2	29.983
3	48.194
4	32.370
5	50.259

The characteristic strength of concrete can be taken value excluding the highest and the lowest value recorded during test. Hence, it can be concluded that the characteristic compressive strength of the bridge can be taken as varying between 29 MPa and 50.2 MPa.

However, according to the Ethiopian Roads Authority bridge design Manual 2013(ERA BSM, 2013) it is stated that the strength of sound concrete shall be assumed to be equal to either the values taken from the plans and specifications or the average of construction test values. When these values are not available, the ultimate stress of sound concrete shall be assumed to be 25 MPa. A reduced ultimate strength shall be assumed (no less than 15 MPa, however) for unsound or deteriorated concrete unless evidence to the contrary is gained by field-testing (ERA Bridge Design Manual, 2013).

In line with the Ethiopian Roads Authority bridge design manual (ERA Bridge Design Manual, 2013), the cubic compressive concrete strength is of 25MPa is used.

CHAPTER 4

FAILURE CRITERIA

Introduction

The behavior and strength of concrete mostly are described as having low tensile strength which results in a tensile crack at a very low tensile stress compared with higher strength in compression. The formation of cracks affects the stiffness of the concrete that give rise to a nonlinear behavior in concrete structures like panel and shells, where developing an accurate and simplified mathematical model is the most important task. Many researchers have developed different linear-elastic fracture models to study the nonlinear response of concrete in structures (Chen and Han,1988).

The strength of concrete under multiaxial stresses is a function of the state of stress and cannot be predicted by the limitation of simple tensile, compressive, and shearing stresses in relation to each other (Wai-Fah, 2014).

Failure criteria a general term in its sense where used for concrete under combined states of stress. In formulating the criteria for concrete, one must come to the physical meaning of failure under a combined state of stress. Different criteria such as yielding, setting of cracking, crushing, and the deformation has been used to define failure. In general, concrete failures can be grouped into tensile and compressive types, characterized by brittleness and ductility, respectively. Tension failure is defined by the formation of major cracks and loss of tensile strength in concrete normal to the crack orientation. In compressive failure, many small cracks develop, and most of the concrete elements lose its strength.

Failure of concrete under general stress has long been based on the well-known coulomb criterion combined with a small tension cutoff. The actual behavior and strength of concrete material are very complex, however, and it depends, among many factors, on the physical and mechanical properties of the components of concrete. Concrete shows many load-carrying capacity values when subject to different conditions. Idealizations are therefore important to develop a simple mathematical model for practical application. (Wai-Fah, 2014).

In this study, simplified failure models or criteria are applied to predict the behavior and strength of concrete under given loading conditions.

Total Strain Crack Model

The tensile behavior of concrete can be modeled using different approaches, one resulting in a more complex description than the other. For the Total Strain crack model, four softening functions based on fracture energy are implemented, a linear softening curve, an exponential softening curve, the nonlinear softening curve according to (Reinhardt et al., and the nonlinear softening curve according to Hordijk, all related to a crack bandwidth as is usual in crack models. Tensile behavior which is directly related to the fracture energy can also be modeled within the Total Strain concept using tension softening function (Midas FEA,2016).

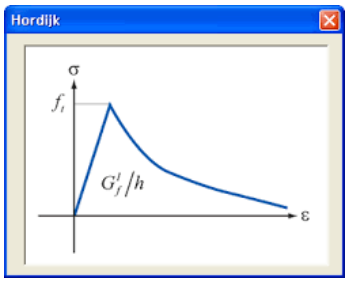

Figure 4-1 Hordijk Tension Softening Curve (Midas FEA, 2016)

The constitutive model for the concrete response to the compression is based on the Thorenfeldt method. The inbuilt function is defined in the software that takes into account the compressive strength of the concrete in the formation of the stiffness matrix (Midas FEA,2016).

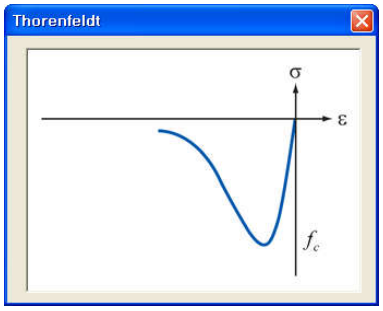

Figure 4-2 Thorenfeldt Compression mode for Concrete (Midas FEA, 2016)

In this study, numerical modeling was carried out by using a commercially available advanced nonlinear finite element program, Midas FEA. The total strain crack model was considered to capture the nonlinear response of concrete under loading.

The total strain crack model implemented in Midas FEA reflects all the ultimate states of materials such as cracking and crushing and shear failure defined through the relationship between shear stress and shear strain. Compressive strength, tensile strength and shear model implemented is defined as thus (Vecchio and Collins, 1986).

The established relation in understanding the behavior of the smeared crack is represented series of micro cracks. After cracking, the elastic modulus of the concrete element is reduced to zero in the direction parallel to the principal tensile stress direction. Crushing occurs when all principal stresses are compressive and lie outside the failure surface; subsequently, the elastic modulus is reduced to zero in all direction normal. This is well illustrated by the powerful features of the Midas FEA software (Midas FEA, 2016).

CHAPTER 5

FEM SIMULATION OF ODIE BRIDGE

In this section, the research approach used to carry out the study is presented. The necessary steps used to carry out the investigations, the assumptions and simplifications used to simulate the realistic site and bridge condition are also discussed in this chapter.

5.1 Finite Element Model Using Midas FEA

The finite element analysis of this study is carried out using a very versatile finite element analysis software for Civil Structures called Midas FEA. This program has a user-friendly interface that enables the creation of the three-dimensional model of the structure to be simulated. The bridge geometry is created in a separate AutoCAD program and imported as dxf (Drawing eXchange Format) file into main Midas FEA software and latter improved using a graphical interface.

The main purpose of generating this model is to study the behavior of the arch in response to the self-weight of the bridge and vehicular moving load. In the analysis, own weight of the bridge is calculated from the material definition and geometry of the structure. The moving load is then applied at a stationery point directly on the critical point based on the influence surface.

5.2 Validation

For Validation purpose, the Prestwood bridge shown in Figure 5-1 is simulated in Midas FEA software and the output is compared with the test result for validation of the model. The bridge is a single-span bridge tested to collapse within the experimental research on masonry bridges supported by the Transport Research Laboratory (Page, 1987).

Prestwood Bridge

The Prestwood bridge is a single-span arch bridge with backfill. The bridge has a uniform arch thickness of 0.22m. The span length of the bridge was 6.55m and with a rise of 1.43m and a fill depth of 0.16m above the crown. The experimental load was applied on a strip of the road surface along the full width of the bridge between the parapets at a point where

the lower load value leading to the failure was expected. The latter has been evaluated by assuming that the arch would fail as a four hinged mechanism and was, then, applied at the quarter-span of the bridge (Page, 1987).

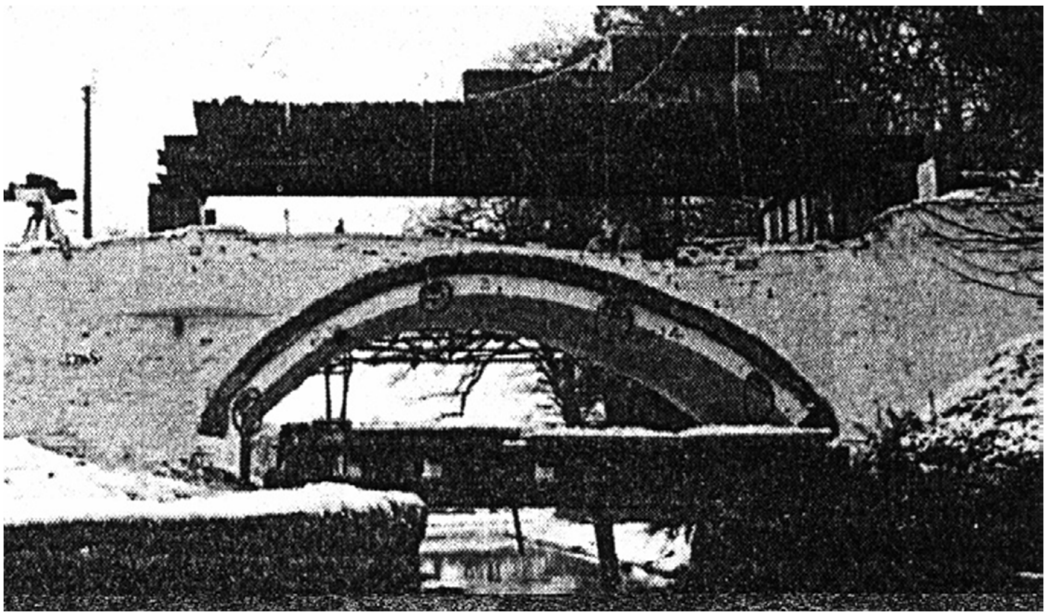

Figure 5-1 Prestwood Bridge before Collapse (Sustainable Bridges SB4.7.3)

The strip was 0.30 m wide to distribute the load and to avoid premature failure of the fill. The load has been applied using hydraulic jacks, while the required reaction for the load was provided by the weight of concrete blocks on a steel frame above the bridge (Figure 5-4). The collapse load was recorded as 228kN that formed four hinges failing by mechanism (Page, J. 1987).

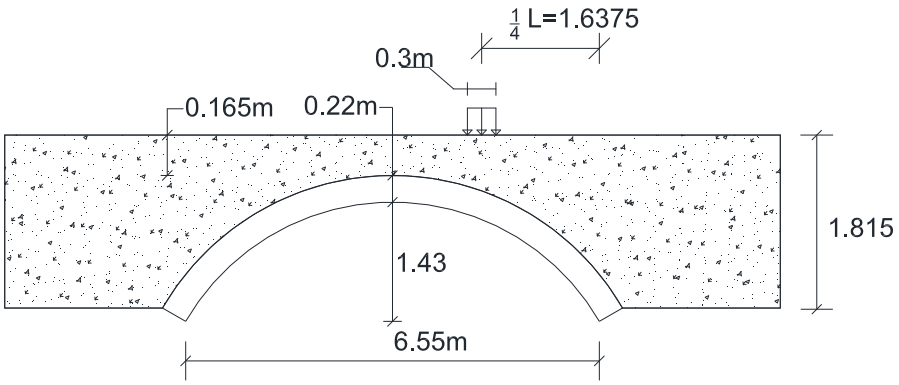

Figure 5-2 Geometry of Prestwood bridge (Page ,1987)

Study of Prestwood Bridge as Total Strain Crack Model

A finite element model of Prestwood bridge was generated for the estimation its load-carrying capacity. The interface between the arch and the fill was modeled using contact friction with a single face contract. The backfill material was idealized as the Mohr-Coulomb model. The boundary conditions were defined as rollers for the backfill and pinned restraints for the arch connection to the foundation. A rigid block with very high stiffness was used to model and simulate the loading apparatus. The analytical model was developed utilizing the material properties of the bridge reported in the TRRL Research Report 110, (Page, 1987).

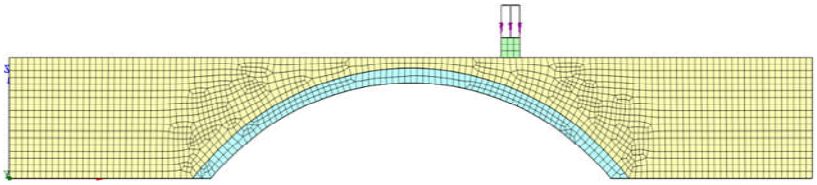

Figure 5-3 FE Model of Prestwood Bridge.

Property / Component	Density	Compressive Strength, fc	E, young's Modulus	Poison's Ratio	The angle of Internal friction	Cohesion
Arch	2040kg/m^3	4.5 N/mm^2	15GPa	0.3	-	-
Backfill	2040kg/m^3	-	0.3GPa	0.3	37	7 kPa

Based on the finite element analysis output, the load that resulted in the formation of the fourth hinge directly under the applied load that leads to mechanism in the bridge is 225kN. This value corresponds to 98% of the collapse load of Prestwood Bridge obtained in the experimental test(228kN). This could be attributed to the fact that the load is in Prestwood bridge is a single load at a fixed position that does not require the use of influence surfaces. It can be concluded that the total strain crack model used to estimate the load carrying capacity of arch bridges and hence similar approach can be used to analyze the Odie bridge.

Figure 5-4 Prestwood Bridge: Mechanism (Page,1987)

The vertical displacement under the test line load was recorded by the acoustic measurement and was reported during the test (Page, 1987). The vertical displacement under the incremental step load in the total strain crack model is plotted and shown in Figure 5-5. The results from the finite element analysis show a close correlation in the vertical displacement up to a load of 150kN.

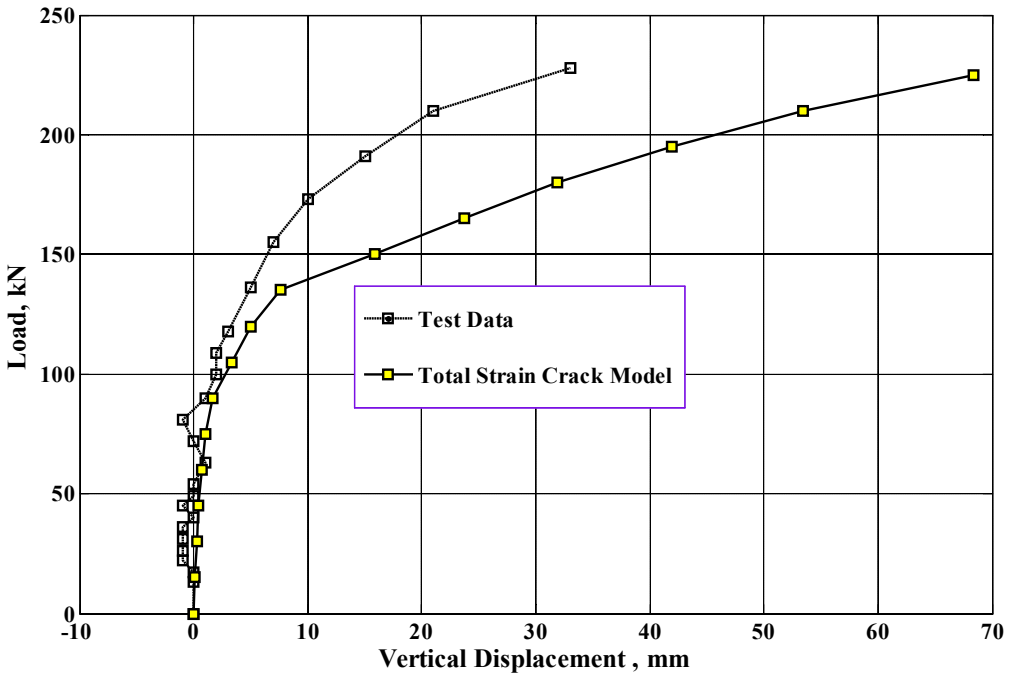

Figure 5-5 Vertical displacements of Point Under loading for Prestwood Bridge

(Positive Displacement shown indicate downward displacement)

5.3 Odie Bridge

The Odie Bridge is drawn in the AutoCAD environment and imported to Midas FEA software.

In Figure 5-6 ,the arch bridge, backfill and boundary conditions are displayed. The finite element model has three parts pavement, arch rib, and backfill. The boundary conditions are assigned to the springing point as pinned, and the backfill is assigned as rollers in the different degrees of freedom.

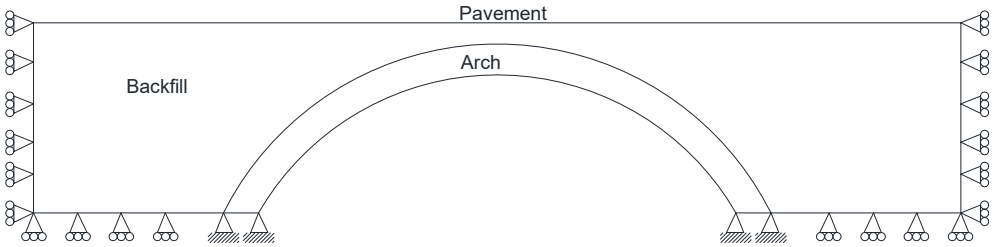

Figure 5-6 Boundary Condition of Odie Bridge

Using the given initial boundary conditions and initial stress conditions, the body force as own weight is activated with moving loads fed to the software, the modeling process ends. The arch and backfill are subjected to concentrated loads at the influence surface points. The moving load is acted to the backfill material that serves as distributing it thought the fill. The load consists of full sets of axles and are subdivided into load steps at equal intervals.

The influence surfaces at different points on the arch are shown in Figure 5-7 to Figure 5-9.

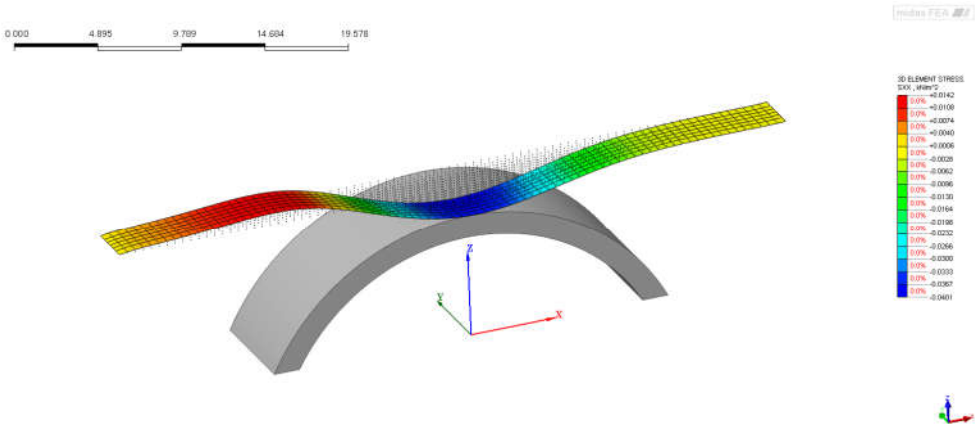

Figure 5-7 Influence surface for solid stress at the Springing point

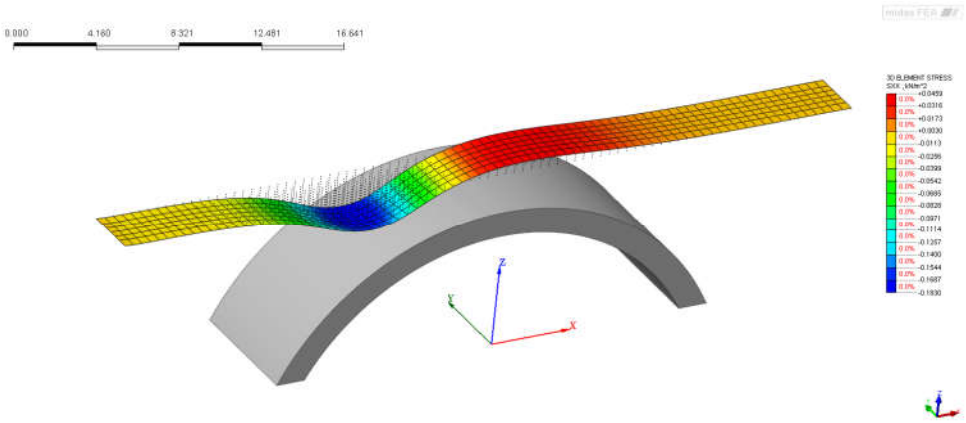

Figure 5-8 Influence surface for solid stress at the Quarter point

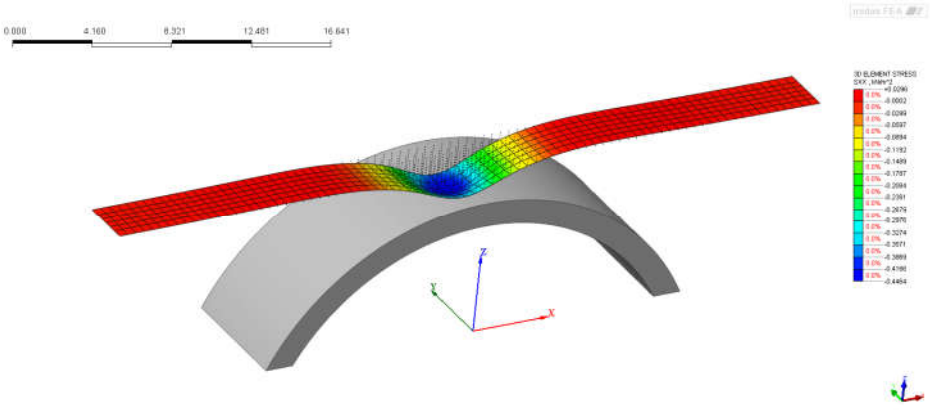

Figure 5-9 Influence surface for solid stress at Crown

The Arch Rib

An 8 node solid elements with mid nodes were used to model the arch rib, backfill, and abutment. The spandrel wall confinement effect was not taken into account due to the strengthening effect of this analysis. The material model that best represents the model is assigned while developing the model.

A finite element analysis requires the division of elements to idealize a real problem to the numerical model. This requires the generation of mesh to suitably discretize in the shape and size of each element in a model and hence the meshing done automatically. However, the quality of the auto-meshed elements is checked and verified to achieve good quality in the results. During the meshing process, a well-organized node-to-node connection is be checked to reduces the computation time that might arise from a very large matrix. Figure 5-10 shows the final discretization of the bridge.

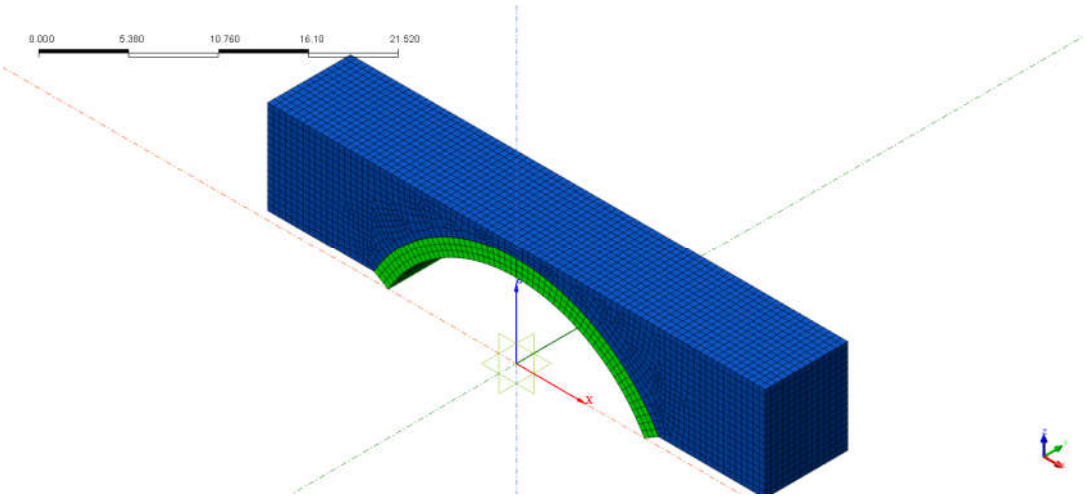

Figure 5-10 Final discretization using Auto-Mesh Finite Element Model of the Bridge

The Backfill

The backfill is considered as an elasto-plastic material with the Mohr-Columb material model. The specification of this model and its yield criterion typically involves Coulomb's theory, which establishes a linear relationship between shear strength on a plane and the normal stress acting on it (Midas FEA,2016, Bowles,1997).

The pavement

The pavement thickness is very small compared to the backfill and the arch and hence its effect in load distribution are insignificant. The pavement load is considered as a distributed load on the top backfill surface.

5.4 Modeling of the Bridge of Odie Bridge

The behavior of concrete under loading is very complex. A non-linear analysis is required to capture the response of concrete under different sets of loads.

To perform the analysis of the model, the following steps are used:

1) Complete geometric generation of the model using line, surface, and solid elements.
2) The arch and the backfill are represented using 8 nodes solid element with node-to-node connectivity that allows smooth shape function between elements in the mesh.

The system of the element, boundary conditions, and node connectivity is sufficiently detailed to properly simulate the complex interaction of the element subjected to a set of loads. This will help to determine the element stress, the crack status, and the crack propagation in the arch section from the applied traffic load.

Material properties in the model

The fracture energy of the concrete G_f, is the energy required to propagate a tensile crack of unit area. According to CEB-FIB Model Code 90, the fracture energy for concrete is $80Nm/m^2$.

Table 5-1 Material Properties of arch Concrete

Arch Concrete	Density	Compressive Strength, fc	Tensile Strength, f_t	E, Young's Modulus	Poison's Ratio	Tensile Fracture Energy, G_f
	$2400kg/m^3$	$20\ N/mm^2$	$1.54N/mm^2$	21.46GPa	0.2	$80Nm/m^2$

(Ethiopian Roads Authority Bridge Design manual, 2013 and CEB-FIP MODEL CODE 1990)

The concrete is modeled as a β-α material with hardening and softening curve as suggested by Thorenfeldt et. al (Midas FEA, 2016). The tension behavior is modeled as non-linear softening using fracture energy. The backfill is modelled as C-ϕ material using Mohr-Coloumb material model (Midas FEA,2016).

Table 5-2 Material Properties of Backfill

	Density	Young Modulus	Poisson's Ratio	Angle of internal friction
Backfill	1800 kg/m^3	0.2GPa	0.30	35°

(Ethiopian Roads Authority Bridge Design manual, 2013 and Bowles,1997)

5.5 Loading

For the assessment of load carrying capacity of the bridge, the legal truck loads shown in Figure 5-11, **Figure 5-12** and Figure 5-13 are used (ERA Bridge Design manual, 2013).

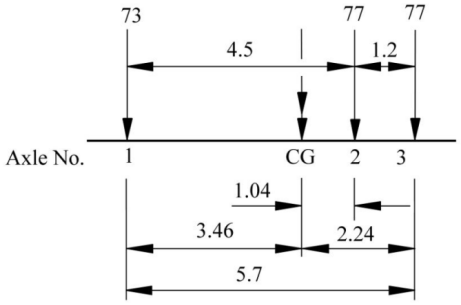

Figure 5-11 Truck Type 3 Unit Weight = 227 kN

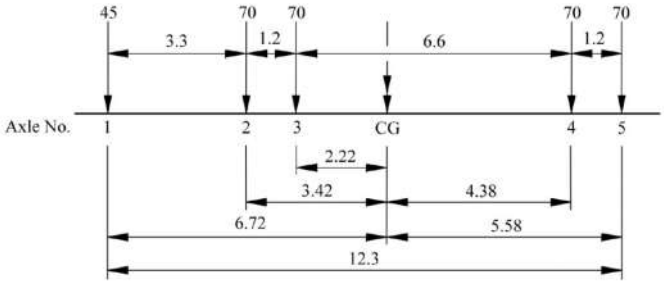

Figure 5-12 Truck Type 3-2 Unit Weight = 325 kN

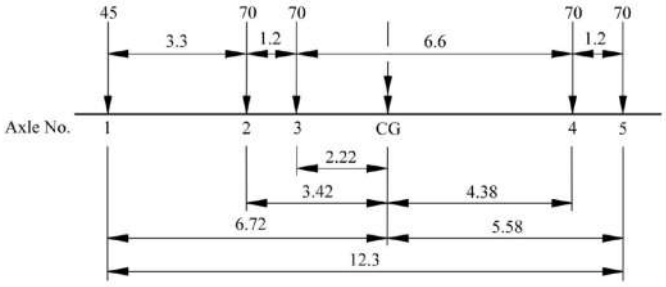

Figure 5-13 Truck Type 3-3 Unit Weight = 364 kN

Impact factor

Impact from the vehicles are included in the analysis for the bridge under investigation. A smooth deck condition is assumed. In this case, an impact factor of 0.1 is used (ERA Bridge Design manual, 2013). The legal truck positions are on Odie Bridge are shown in Figure 5-14 to Figure 5-17.

5.6 Analysis

In the analysis steps following two stages are used

1) The response of the bridge from its own weight will be analyzed and stored for the next stage
2) The bridge is analyzed to check its response towards the formation of the first hinge mechanism and the load that causes it to go into a mechanism. In this case the maximum load that causes plastic hinge is obtained.

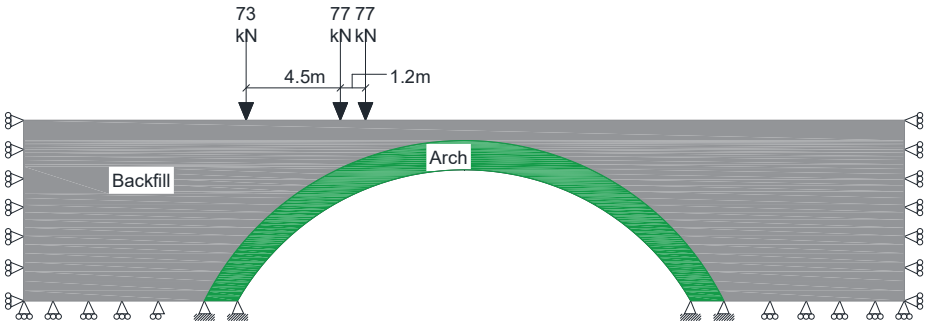

Figure 5-14 Loading at Quarter Point, Legal Truck Type-3

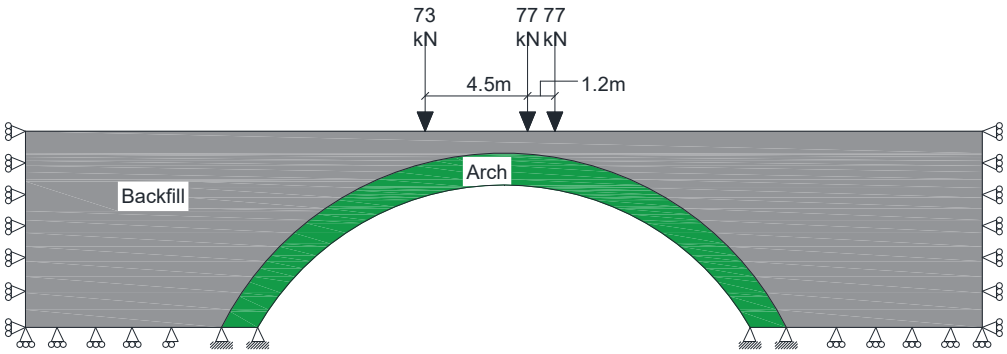

Figure 5-15 Loading at Crown, Legal Truck Type-3

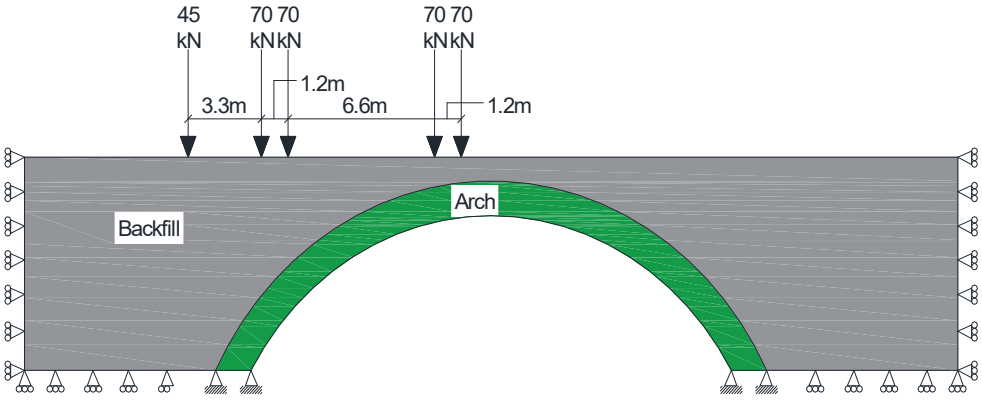

Figure 5-16 Loading at Quarter Point, Legal Truck Type-3-2

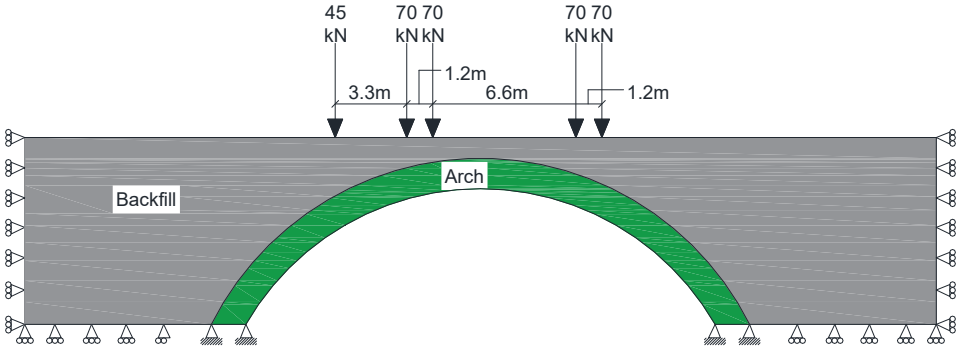

Figure 5-17 Loading at Crown, Legal Truck Type-3-2

Analysis solution

In nonlinear analysis, the total load applied to a finite element model is divided into a series of load increments called load steps. At the completion of each incremental solution, the stiffness matrix of the model is adjusted to reflect nonlinear changes in structural stiffness before proceeding to the next load increment. The Midas FEA has an iteration procedure for find solution. Newton–Raphson equilibrium iterations for updating the model stiffness. In this study, for the concrete solid elements, convergence criteria were based on energy, and the convergence tolerance limits were based on the default set by the program. It was found that convergence of solutions for the models was difficult to achieve due to the nonlinear behavior of reinforced concrete. Therefore, the convergence tolerance limits were increased to a maximum of 0.1 which is 10 times default tolerance limits (0.01) to obtain convergence of the solutions.

CHAPTER 6

RESULT and DISCUSSION

Mainly the analysis is targeting in finding the crack pattern and its growth for the selected section that changes its material properties as the stress in each section changes depending on the material non-linearity defined in the modeling process.

The stress in the arch responding in a non-linearly for each load step is defined as the moving traffic load. The crack growth and its orientation are fixed in the material model and hence the definition of the section for failure is carefully investigated for its effect in the length and extent of the crack. As the stress in the arch increase with cumulating loadings at consecutive load steps the crack opens and reaching the outermost section of the arch will be reported as the highest load that creates a hinge in the cross section. Here the maximum load that the arch can sustain just before the collapse is the one which caused all the four hinges to form.

From the analysis for legal truck type 3, the first hinge was formed at the quarter point of the arch under the center of gravity of the axles with corresponding load of 2824.87kN. The second hinge formed at the springing point with corresponding load of 4622.52kN. The third hinge and the fourth hinge formed with corresponding load of 6163.36kN and 6933.78kN respectively. The locations of the plastic hinges are shown in Figure 6-1 to Figure 6-7. Moreover, the load-displacement diagram of the first hinge at the quarter point on arch is shown in Figure 6-5.

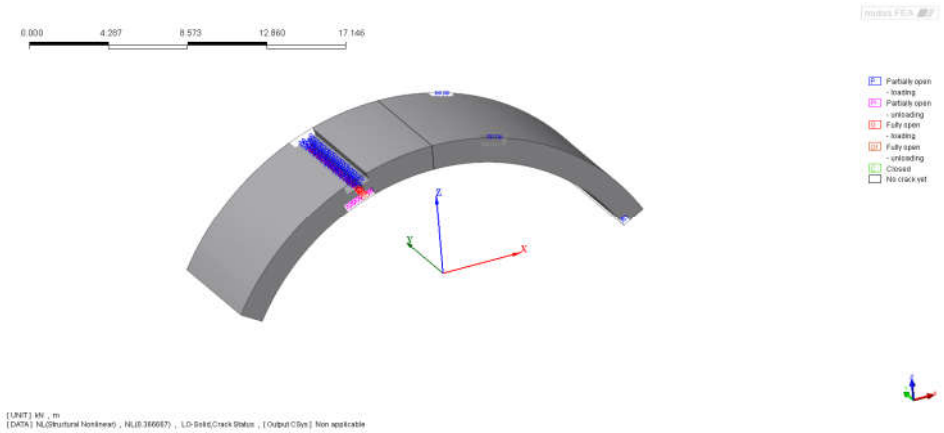

Figure 6-1 Hinge No.1 at Quarter Point, Legal Truck Type 3, Total Axle Load= 2824.87kN at 11th Load step

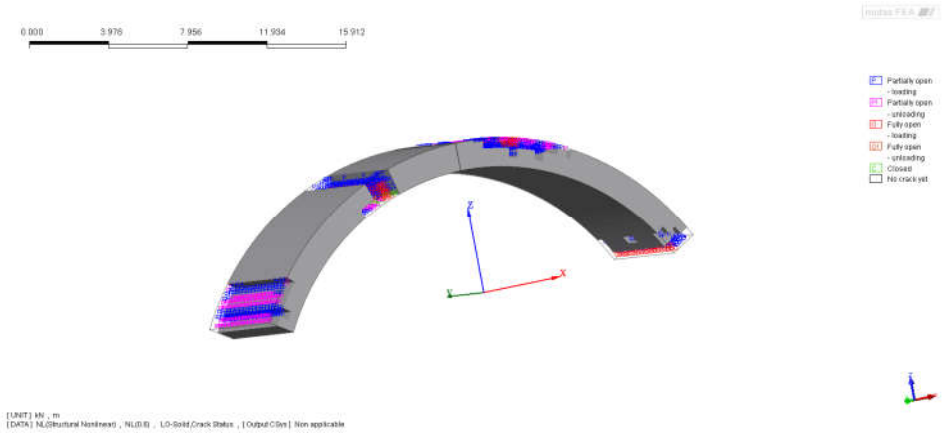

Figure 6-2 Hinge No.2 at Right Springing Point, Legal truck Type 3, Total Axle Load=4622.52 kN at 18th Load step

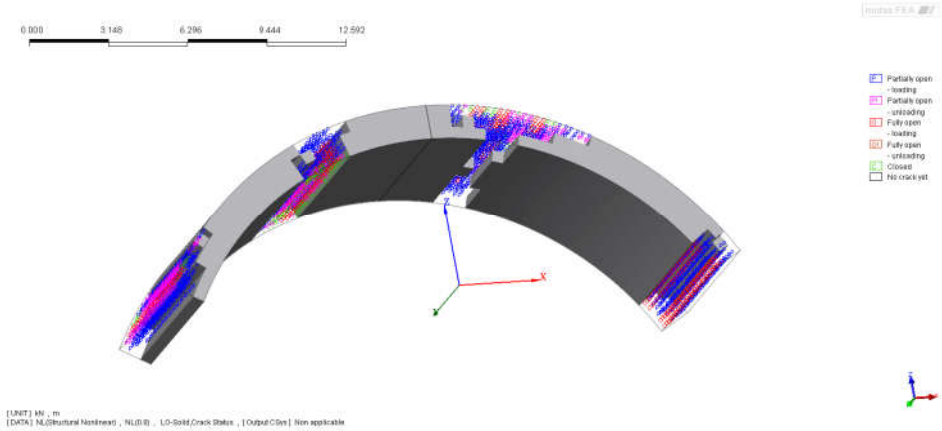

Figure 6-3 Hinge No.3 at Three Quarter Point, Legal truck Type 3, Total Axle Load=6163.36 kN at 24th Load step

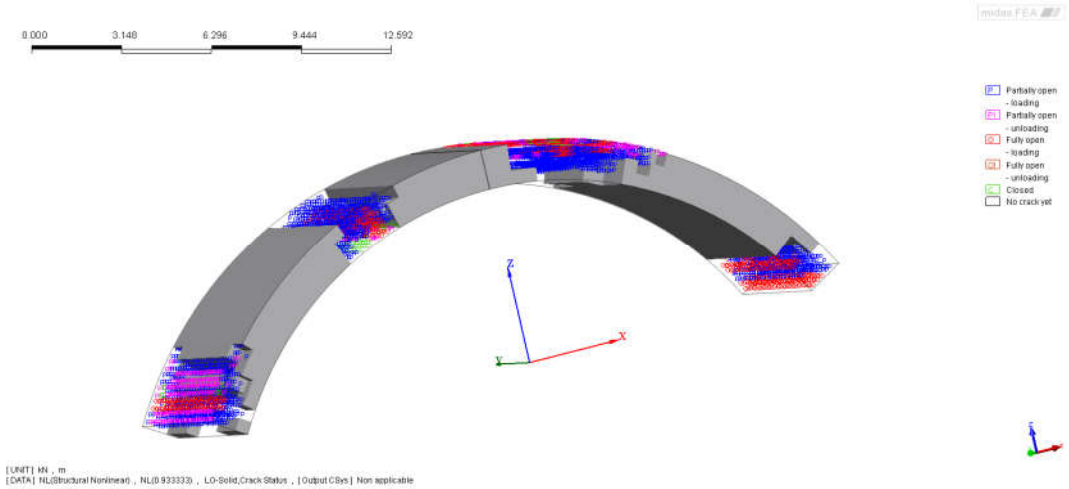

Figure 6-4 Hinge No.4 at Left Springing Point, Legal truck Type 3, Total Axle Load=6933.78kN at 27th Load step

The vertical displacement of the in Figure 6-5 shows that at the formation of the first hinge the displacement value shows a sudden increase for a very small load increment.

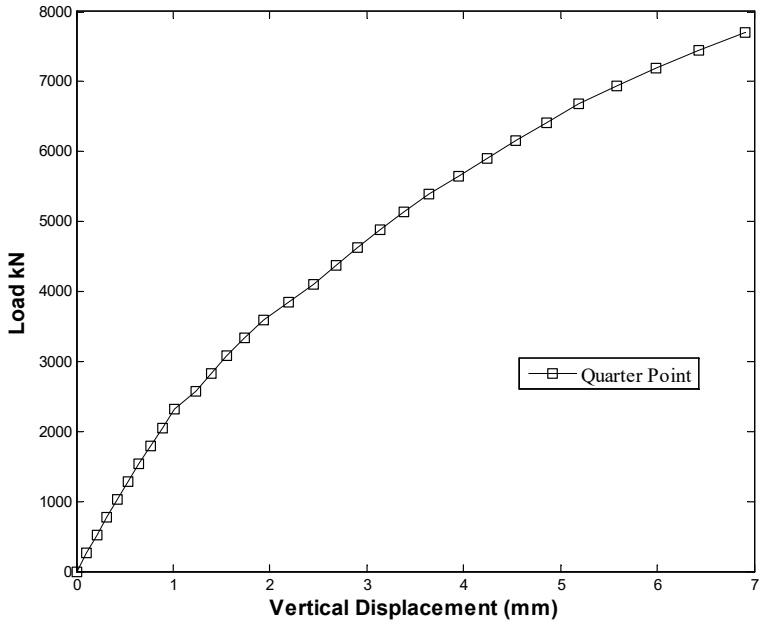

Figure 6-5 Vertical Displacement of quarter-point on arch under the Load for Legal Truck Load type 3

The load before the formation of the first hinge can be taken as the safest load that the arch can sustain. In this case, 2824.87kN is the maximum total axle load Odie Bridge can carry.

Based on the recommendations given, the rating factor (safety factor) is computed using the following equation (Eq 6-1):

$$RF = \frac{\emptyset R_n - \sum_{i=1}^{m} \gamma_i^D \times D_i - \sum_{i=1}^{n} \gamma_j^L L_j (1 + I)}{\gamma^{LR} L_R (1 + I)} \qquad \textbf{Eq 6-1}$$

(ERA BDM,2013)

Where: RF = rating factor (the portion of the rating Legal Truck allowed on the bridge)

ϕ = resistance factor

m = number of elements included in the dead load

Rn = nominal resistance

n = number of live loads other than the rating vehicle

γiD= dead load factor for element "i"

Di = nominal dead load effect of element "i"

γjL= live load factor for live load "j" other than the rating vehicle(s)

Lj = nominal traffic live load effects for load "j" other than the rating vehicle(s)

γLR= live load factor for rating Legal Truck

LR = nominal live load effect for the rating Legal Truck

I = live load impact factor

Hence, the rating factor of Odie bridge for the legal truck type 3 is 3.14.

Similarly, the legal truck was positioned at the crown and the results of this configuration first hinge formed with corresponding load of 6676.97kN. The second hinge formed at the springing point with corresponding load of 13353.97kN. Hence, the third and the formation of the fourth hinge were irrelevant as the second hinge formed for load the crown is far greater than the formation of a fourth hinge in the load positioned at the quarter-point for the legal truck type 3. The locations of the plastic first and second hinges are shown in Figure 6-6 and Figure 6-7.

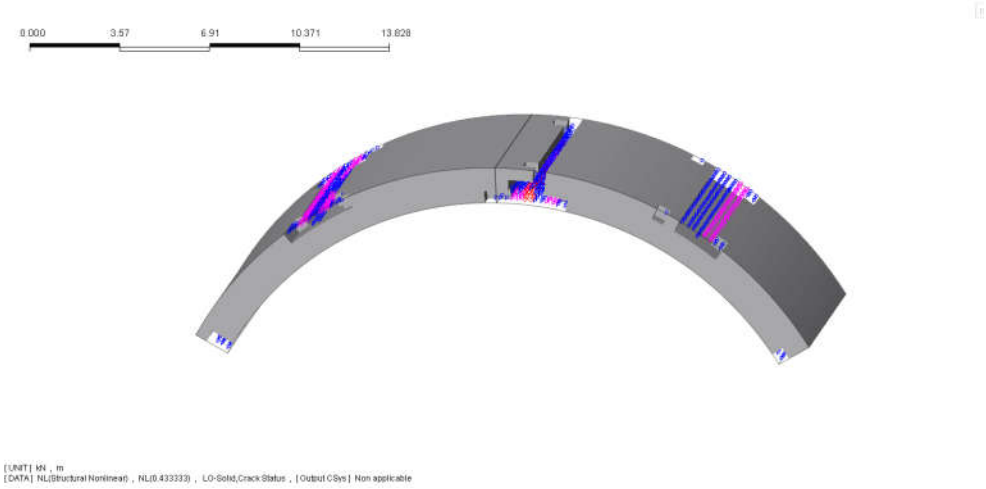

Figure 6-6 Hinge No.1 at Load at Crown, Legal Truck Type 3, Total Axle Load=6676.97kN at 13th Load step

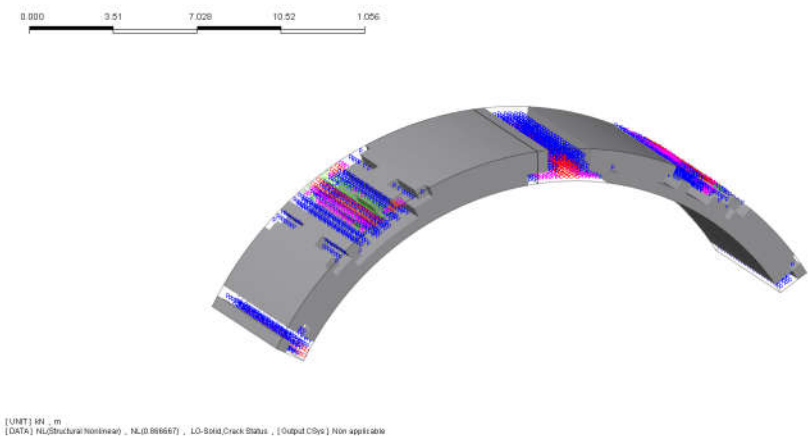

Figure 6-7 Hinge No.2 at Springing, Legal Truck Type 3, Total Axle Load= 13353.97kN at 26th Load step

With regard to this, the quarter-point loading is more critical than the crown point loading. Hence, the load carrying capacity of the is controlled by the quarter point loading with capacity to sustain 6676.973kN with a rating factor (safety factor) of 7.42 based on Eq 6-1.

Due to the loading arrangement and spacing of the axles the legal truck type 3-2 is not the critical vehicle type for the case study. The first hinge formed at the quarter-point at a total axle load of 53539.158kN. This load is unrealistically very high due to the balancing effect of the axle arrangement on the influence surface and the arch thickness being very large.

CHAPTER 7

CONCLUSIONS AND RECOMMENDATIONS

7.1 Conclusion

Arch bridges show rather complex behavior when subjected any loading condition especially under moving traffic loading. Based on the research conducted, the following conclusions are drawn,

- Odie Bridge can carry a maximum total axle load of 282ton with the least favorable condition (Legal Type 3).
- The methodology proposed for the evaluation of the load carrying capacity of arch bridge is a more realistic and a good approximation.
- In the absence of as built drawings and detailed test data, estimation of load carrying capacity of arch bridges is difficult.

7.2 Recommendation

- In the assessment of arch bridges, spandrel walls should be considered.
- The effect of seismic and environmental loads needs to be considered for future study.

REFERENCES

Blake L S. (2001) Civil Engineer's Reference book 4th Edition, Butterworth-Heinemann, Linacre House, Jordan Hill, Oxford.

Bowles Joseph E., RE., S. (1997), Foundation Analysis and Design (5th Edition), McGraw-Hill, Singapore

Brencich A & de Francesco U (2004) Assessment of Multispan Masonry Arch Bridges: Simplified Approach. ASCE Journal of Bridge Engineering.

Bridle, R. J. and Hughes T. G. ,(1990) "An energy method for arch bridge analysis." Proc. Inst. Civ. Engrs, London.

C.E.I.D.B. (1990), 'CEB-FIB Model Code 1990: Design Code, Thomas Telford Services Ltd, Switzerland

EN 1992-1-1:2004 (2004), Eurocode 2: Design of concrete structures. Part 1: General rules and rules for buildings. European Committee for Standardization, Brussels

EN206-1-Part 1(2000): Specification, performance, production, and conformity. European Committee for Standardization, Brussels.

ERA BDM, Bridge Design Manual, (2013), Ethiopian Roads Authority, Ethiopia.

ERA BMS: ERA Bridge Management System (BMS), (2010), Ethiopian Roads Authority, Ethiopia.

Heyman J .(1966) The stone skeleton. Structural Engineering of Masonry Architecture, University of Cambridge, Cambridge.

Highway structures: Inspection and maintenance Assessment of highway bridges and structures. (2001) DMRB Volume 3 Section 4 Part 4 (BA 16/97). Highway Agency, London: HMSO.

Martín-Caro JA & Martínez LJ (2004) A first-level structural analysis tool for the Spanish Railways Masonry Arch Bridges. Arch Bridges IV – Advances in Assessment, Structural Design, and Construction, P Roca & C Molings (Eds), CIMNE, Barcelona, pp 192–201

Midas FEA (2016). User manual version 2016, Midas IT, Seuol, South Korea

Page, J. (1987). Load tests to collapse on two arch bridges at Preston, Shropshire, and Prestwood, Staffordshire. Crowthorne, England.

Pippard A. J. S. (1948) "The approximate estimation of safe loads on masonry bridges." Civil Engineer in War, Vol 1, 365. Inst. Civ. Engrs, London.

Qian, L. X. (1987). The carrying capacity of Zhao Zhou stone arch bridge. J. Chinese Civil Engineering., 4, pp. 831-843

Selby, R.G, and Vecchio, F.J. (1993) 3D Constitutive Relations for Reinforced Concrete, Tech, Rep.93-02, Department of Civil Engineering, Toronto, Canada

Steinman, D. B., and Watson, S.R. (1941). Bridge and Their Builder, G.P. Putnam's Sons, New York, NY.

Sustainable Bridge SB4.7.3, (2007), Methods of analysis of damaged masonry arch bridges, Background document, Sustainable Bridges.

Vecchio, F.J., and Collins, M.P. (1986) 'The Modified compression field theory for reinforced concrete elements subjected to shear', ACI Journal 83,22, 219-231.

Wai-Fah Chen and Han D.J (1988). Plasticity for Structural Engineers, Springer-Verlag, New York, NY.

Wai-Fah Chen and Lian Duan. (2014) Bridge Engineering Handbook-Superstructure Design, Second Edition, CRC Taylor & Francis Group.

APPENDIX A

Estimation of Concrete Strength from the Schmidt Hammer Test

The summary of sample sets at different representative spots on the arch rib

At Springing Left Abutment 1

Count/Tests	Rebound	Compressive Strength (MPa)	Mean	x-mean	$(x\text{-mean})^2$	Standard Deviation
1	56	73	77	-4.000	16.000	6.923
2	58	77		0.000	0.000	
3	56	73		-4.000	16.000	
4	56	73		-4.000	16.000	
5	64	89		12.000	144.000	

Characteristic Strength as per EN 206-1:2000 at 65.63MPa

At Springing Right Abutment 1

Count/Tests	Rebound	Compressive Strength (MPa)	Mean	x-mean	$(x\text{-mean})^2$	Standard Deviation
6	34	31	42.4	-11.400	129.960	7.569
7	42	45		2.600	6.760	
8	46	52		9.600	92.160	
9	40	42		-0.400	0.160	
10	40	42		-0.400	0.160	

Characteristic Strength as per EN 206-1:2000 at 29.98MPa

At Springing Left Abutment 2

Count/Tests	Rebound	Compressive Strength (MPa)	Mean	x-mean	$(x\text{-mean})^2$	Standard Deviation
11	44	49	65.8	-16.800	282.240	10.733
12	52	65		-0.800	0.640	
13	52	65		-0.800	0.640	
14	56	73		7.200	51.840	
15	58	77		11.200	125.440	

Characteristic Strength as per EN 206-1:2000 at 48.19MPa

At Springing Right Abutment 2

Count/Tests	Rebound	Compressive Strength (MPa)	Mean	x-mean	$(x\text{-mean})^2$	Standard Deviation
16	36	34	43	-9.000	81.000	6.480
17	40	42		-1.000	1.000	
18	40	42		-1.000	1.000	
19	42	45		2.000	4.000	
20	46	52		9.000	81.000	

Characteristic Strength as per EN 206-1:2000 at 32.37MPa

At Quarter Point Left

Count/Tests	Rebound	Compressive Strength (MPa)	Mean	x-mean	$(x\text{-mean})^2$	Standard Deviation
21	57	57	61.6	-4.600	21.160	6.913
22	52	52		-9.600	92.160	
23	65	65		3.400	11.560	
24	65	65		3.400	11.560	
25	69	69		7.400	54.760	

Characteristic Strength as per EN 206-1:2000 at 50.26MPa

APPENDIX B

Arch bridge Design Procedure

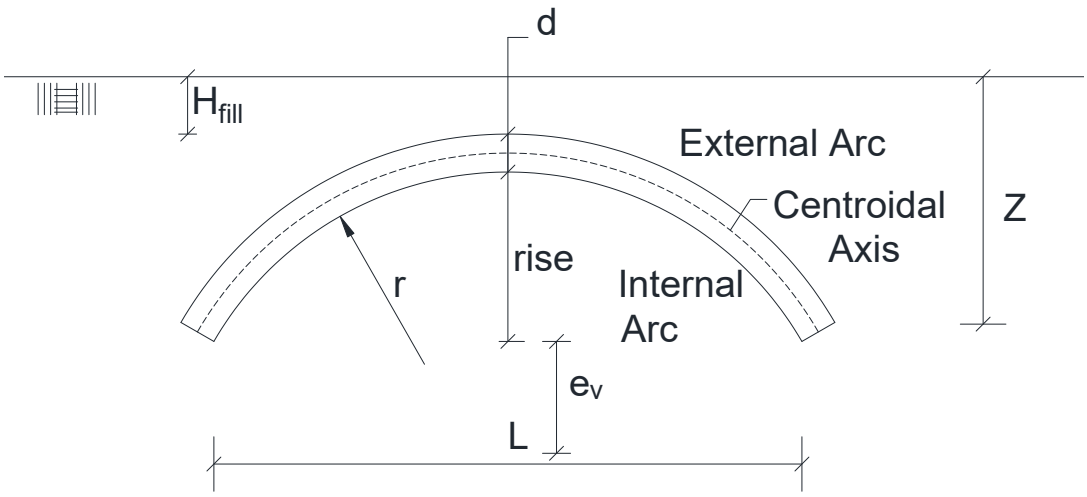

Figure Dimensions of Arch

L-Span of arch

Rise-rise of arch

H_{fill}-height of fill above the crown

Z- is the total height to top of the fill

r-is radius of the arch

f'c-compressive strength of concrete

E-modulus of elasticity of arch material

γ_c -density of concrete

γbf-density of fill material

γ_{SM}-density of stone masonry

d-is arch thickness

Flow chart for an arch bridge design

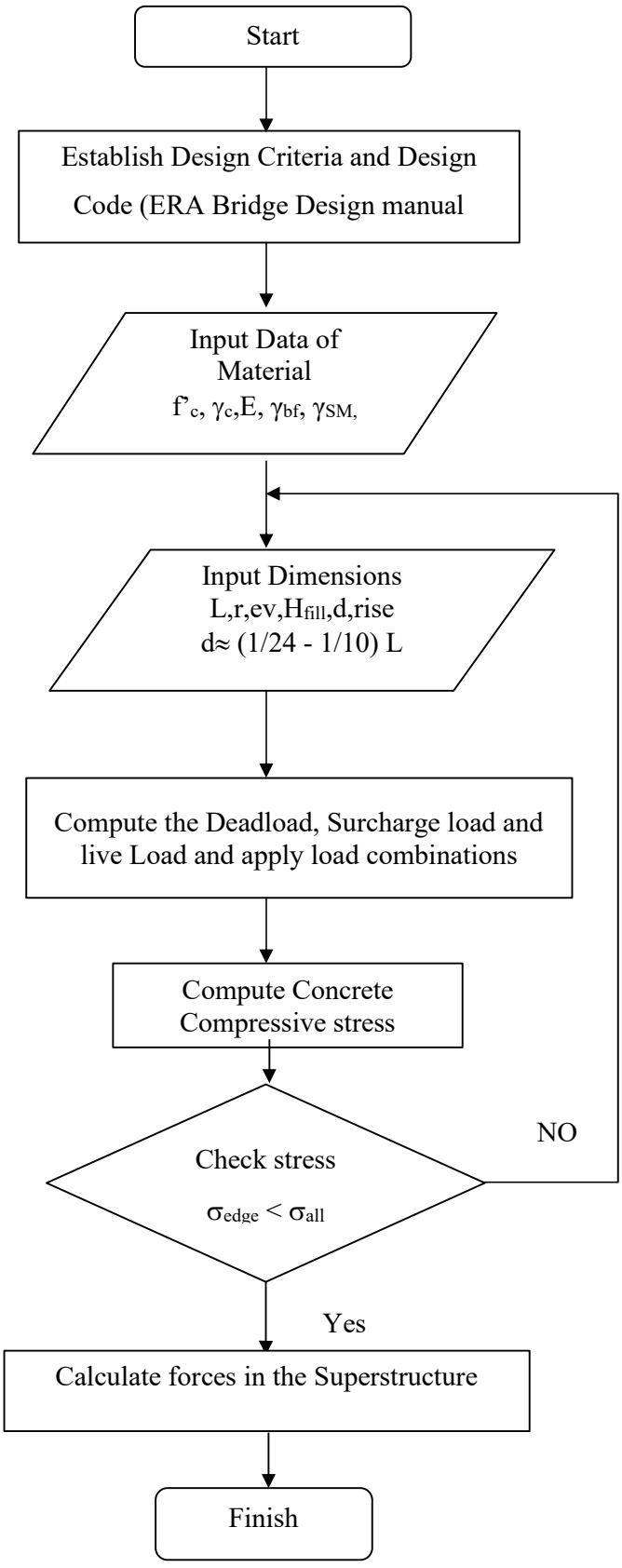

1. Choose span and rise.
2. Select materials to be used.
3. Determine trial section using a selection of empirical equations.
4. Ignoring horizontal soil pressures, calculate the required arch barrel thickness using a simple 'block' mechanism for the ultimate load condition. This can be assumed to comprise of appropriately factored loading.
5. Check the compressive stress based on 0.1 (arch thickness) or 100 mm whichever is the greater. Compressive stress $\leq \lambda_u f$

   where λ_u is a coefficient of 0.35 for concrete grades 15 and 20, 0.4 for concrete grades 25 and above, and 0.44 for masonry; f is the characteristic cube strength of concrete, f_{cu}, or the compressive strength of masonry f_K as appropriate (allowance for γ_M has been made).
6. Check that the radial shear at the crown is less than 0.4 (horizontal reactions).
7. Check abutment stability and stress levels.
8. Check foundation stability and stress levels.

APPENDIX C

Load subdivisions (Legal Truck Type 3) for Quarter Point Loading

Load Step	Divisions	Total Axle load (kN),
1	0.03	256.80
2	0.06	513.61
3	0.10	770.42
4	0.13	1027.22
5	0.16	1284.03
6	0.20	1540.84
7	0.23	1797.64
8	0.26	2054.45
9	0.30	2311.26
10	0.33	2568.06
11	**0.36**	**2824.87**
12	0.40	3081.68
13	0.43	3338.48
14	0.46	3595.29
15	0.50	3852.1
16	0.53	4108.90
17	0.56	4365.71
18	**0.60**	**4622.52**
19	0.63	4879.32
20	0.66	5136.13
21	0.70	5392.94
22	0.73	5649.74
23	0.76	5906.55
24	**0.80**	**6163.36**
25	0.83	6420.16
26	0.86	6676.97
27	**0.90**	**6933.78**
28	0.93	7190.58
29	0.96	7447.39
30	1.00	7704.2

APPENDIX D

Load subdivisions (Legal Truck Type 3) for Crown Point Loading

Load Step	Divisions	Total Axle load (kN),
1	0.03	513.61
2	0.06	1027.22
3	0.10	1540.84
4	0.13	2054.45
5	0.16	2568.06
6	0.20	3081.68
7	0.23	3595.29
8	0.26	4108.90
9	0.30	4622.52
10	0.33	5136.13
11	0.36	5649.74
12	0.40	6163.36
13	**0.43**	**6676.97**
14	0.46	7190.58
15	0.50	7704.2
16	0.53	8217.81
17	0.56	8731.42
18	0.60	9245.04
19	0.63	9758.65
20	0.66	10272.27
21	0.70	10785.88
22	0.73	11299.49
23	0.76	11813.11
24	0.80	12326.72
25	0.83	12840.33
26	**0.86**	**13353.95**
27	0.90	13867.56
28	0.93	14381.17
29	0.96	14894.79
30	1.00	15408.40